

**PERFORMANCE EVALUATION OF CARRIER-LESS AMPLITUDE
PHASE MODULATION SCHEME FOR INDOOR VISIBLE LIGHT
COMMUNICATION (VLC) SYSTEM**

JOYCE YEW PEI LING



UNIVERSITI TEKNIKAL MALAYSIA MELAKA

**PERFORMANCE EVALUATION OF CARRIER-LESS
AMPLITUDE PHASE MODULATION SCHEME FOR INDOOR
VISIBLE LIGHT COMMUNICATION (VLC) SYSTEM**

JOYCE YEW PEI LING

**This report is submitted in partial fulfilment of the requirements
for the degree of Bachelor of Electronic Engineering with Honours**



**Faculty of Electronics and Computer Engineering
Universiti Teknikal Malaysia Melaka**



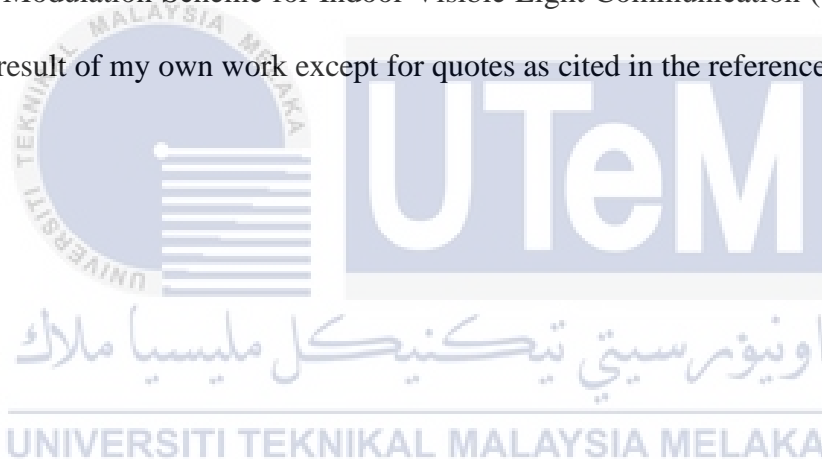
اونيورسيتي تيكنيكل مليسيا ملاك

UNIVERSITI TEKNIKAL MALAYSIA MELAKA

2022

DECLARATION

I declare that this report entitled "Performance Evaluation of Carrier-less Amplitude Phase Modulation Scheme for Indoor Visible Light Communication (VLC) System" is the result of my own work except for quotes as cited in the references.



Signature :

Author : JOYCE YEW PEI LING

Date : 14/01/2022.....

APPROVAL

I hereby declare that I have read this thesis and, in my opinion, this thesis is sufficient in terms of scope and quality for the award of Bachelor of Electronic Engineering with Honours.



اونيورسيتي تيكنيكل مليسيا ملاك

Signature :

UNIVERSITI TEKNIKAL MALAYSIA MELAKA

Supervisor Name : Ts Dr Zaiton Abdul Mutalip

Date : 14 January 2022

DEDICATION

To: My beloved parents. My sister



ABSTRACT

According to recent trends, the existing radio frequency (RF) spectrum may be insufficient to fulfill future data demands. The use of visible spectrum for wireless transmission in visible light communication may be a possible alternative to the RF 'Spectrum Crunch.' Investigating the performance of various modulation techniques in VLC is a new field of research. In the VLC system, data is transmitted digitally and represented by turning ON/OFF the LED. Basically, this is done by a modulator. However, based on the evolution of new generation high brightness LED's, the LEDs intensity and flickering become the major problem in VLC, which limits the transmission bandwidth and the performance of the system. This project examines carrier-less amplitude phase (CAP) modulation techniques to overcome this problem and proposes a suitable improvement to the system to be used. Within a simulated VLC system, the performance of CAP in terms of eye diagram, BER and scatter plot is examined. The BER for CAP is zero as no distance is set in simulation which allows perfect transmission to be simulated. For scatter plots, it can be observed that as the CAP modulation number increases, the scatter plot also increases. For eye diagram, it was noted that CAP modulation offers a better visual representation of how noise could affect system performance than OOK modulation.

ABSTRAK

Mengikut perkembangan terkini, spektrum frekuensi radio (RF) sedia ada mungkin tidak mencukupi untuk memenuhi permintaan data masa hadapan. Penggunaan spektrum untuk penghantaran wayarles dalam komunikasi cahaya boleh dilihat mungkin merupakan alternatif yang mungkin kepada RF 'Spectrum Crunch'. Kajian prestasi pelbagai teknik modulasi dalam VLC adalah bidang penyelidikan baharu. Dalam sistem VLC, data dihantar secara digital dan diwakili dengan menghidupkan atau mematikan LED. Pada asasnya, ini dilakukan oleh pemodulat. Walau bagaimanapun, berdasarkan evolusi LED kecerahan tinggi generasi baharu, keamatan dan kelipan LED menjadi masalah utama dalam VLC, yang menghadkan lebar jalur penghantaran dan prestasi sistem. Projek ini mengkaji teknik modulasi fasa amplitud tanpa pembawa (CAP) untuk mengatasi masalah ini dan mencadangkan penambahbaikan yang sesuai kepada sistem yang akan digunakan. Dalam sistem VLC simulasi, prestasi CAP dari segi 'eye diagram', 'BER' dan 'scatter plot' diperiksa. Untuk 'eye diagram', diperhatikan bahawa modulasi CAP menawarkan gambaran visual yang lebih baik tentang bagaimana bunyi boleh menjejaskan prestasi sistem berbanding modulasi OOK. 'BER' untuk CAP adalah sifar kerana tiada jarak ditetapkan dalam simulasi yang membolehkan

penghantaran sempurna disimulasikan. Bagi 'scatter plot', dapat diperhatikan bahawa apabila nombor pemodulat CAP meningkat, plot serakan juga meningkat.



ACKNOWLEDGEMENTS

I would like to offer my heartfelt gratitude to everyone who made it possible to complete this report. In addition, Ts Dr Zaiton Abdul Mutalip, my Final Year Project (FYP) supervisor, deserves special thanks for her stimulating recommendations and guidance. When I came into a snag or had a question regarding my research or writing, Dr Zaiton's office door would always be open. She continually let me work on this paper, but she always pointed me in the proper path when she felt I needed it.



In addition, I'd want to recognise the critical role played by all of the staff who allowed us to use all of the essential equipment and resources to finish this job. Last but not least, credit to the PSM Committee for devoting their time and effort to assisting the student in completing the FYP. I would like to recognise the support of other supervisors and panels, particularly during this project's presentation, since their criticisms and recommendations helped me improve my presentation skills.

TABLE OF CONTENTS

Declaration	
Approval	
Dedication	
Abstract	i
Abstrak	ii
Acknowledgements	iv
Table of Contents	v
List of Figures	viii
List of Tables	x
List of Symbols and Abbreviations	xi
List of Appendices	xiii
CHAPTER 1 INTRODUCTION	1
1.1 Background	1
1.2 Problem Statement	4
1.3 Objective of the project	5
1.4 Scope of the Project	5

1.5	Thesis Outline	5
CHAPTER 2 LITERATURE REVIEW		7
2.1	Introduction	7
2.2	Visible Light Communication	7
2.2.1	Comparison of RF-based links and VLC technology	8
2.2.2	VLC's potential	11
2.2.3	VLC's drawbacks	12
2.3	Modulation schemes for VLC	12
2.3.1	On-off keying (OOK)	13
2.3.2	Carrier-Less Amplitude Phase (CAP) Modulation	15
2.4	Light Sources	24
2.4.1	Light Emitting Diode	25
CHAPTER 3 METHODOLOGY		27
3.1	Introduction	27
3.1.1	System Flow Chart	28
3.2	Implementation of the system parameters	29
3.3	VLC system coding	31
3.3.1	Room parameters simulation coding	31
3.3.2	Coding to calculate the LOS channel gain	34
3.3.3	Illumination Distribution	35

3.4	OOK Modulation	36
3.5	CAP modulation	38
CHAPTER 4 RESULTS AND DISCUSSION		44
4.1	VLC Simulation Result	44
4.2	Performance Evaluation	49
4.2.1	BER analysis	49
4.2.2	Scatter Plot analysis	51
4.2.3	Eye Diagram analysis	54
4.3	Comparison Between CAP and OOK modulation	56
4.4	Applications & Commercialization Potential	58
4.5	Sustainability & Environmentally Friendly	58
CHAPTER 5 CONCLUSION AND FUTURE WORKS		59
5.1	Conclusion	59
5.2	Future Work	61
REFERENCES		62
LIST OF PUBLICATIONS AND PAPERS PRESENTED		68
APPENDICES		69

LIST OF FIGURES

Figure 1: Frequency spectrum of the visible light spectrum in electromagnetic [6]	3
Figure 2: Block diagram of a VLC system.[1]	8
Figure 3: OOK modulation	14
Figure 4: CAP transmission system's basic architecture [21]	16
Figure 5: Basic CAP systems	18
Figure 6: Functioning of Semiconductor Devices	25
Figure 7: System flow chart	28
Figure 8: CAP-2 scheme	38
Figure 9: Eye diagram scope and scatter plot Connection	39
Figure 10: Transmitted and received pulse	40
Figure 11: Error Rate Calculation block	40
Figure 12: BER graph for CAP-2 without delay	41
Figure 13: Block diagram for QAM modulation and demodulation and random integer generator	42
Figure 14: Power meter connection	43
Figure 15: LED array and distribution of illuminance for a single transmitter	44
Figure 16: Performance graphs of SNR	46
Figure 17: SNR Distribution in the room	47
Figure 18: Pattern of illumination for a single LED transmitter	48

Figure 19: Received power distribution	49
Figure 20: BER graph for (a) OOK Mod, (b) CAP-2, (c) CAP-4, (d) CAP-8	50
Figure 21: Scatter Plot for (a) OOK Mod, (b) CAP-2, (c) CAP-4, (d) CAP-8	51
Figure 22: Scatter plot for CAP-2 with signal quality measurement	52
Figure 23: Eye diagram for (a) OOK Mod, (b) CAP-2, (c) CAP-4, (d) CAP-8	55
Figure 24: QAM's Constellation diagram	56



LIST OF TABLES

Table 1: Global Mobile Data Traffic, 2016–2021[6]	9
Table 2: Comparison between RF-based link and VLC technology	10
Table 3a: Experiments demonstrating the transmission of data via CAP in VLC systems [37]	20
Table 4: A comparison of performance evaluation of the relative advantages of modern modulation formats [37].	24
Table 5: Main simulation Parameters	29
Table 6: Comparison of the Modulation scheme for EVM, MER and Output Power	53
Table 7: Bit per Symbol comparison	57

LIST OF SYMBOLS AND ABBREVIATIONS

BER	:	Bit Error Rate
CAP	:	Carrier-Less Amplitude Phase
DC	:	Direct Current
DD	:	Direct Detection
DMT	:	Discrete Multitone
EVM	:	Error Vector Magnitude
FIR	:	Finite Impulse Response
FOV	:	Field of View
FSO	:	Free-Space Optical
HPF	:	High Pass Filter
IM	:	Intensity Modulation
IoT	:	Internet-of-Things
LED	:	Light Emitting Diode
LOs	:	Local Oscillators
MER	:	Modulation Error Ratio
OOK	:	On-Off Keying
OWC	:	Optical Wireless Communications
PAPR	:	Peak-to-Average Power Ratio
PD	:	Photodetector

QAM	:	Quadrature Amplitude Modulation
QAM	:	Quadrature Amplitude Modulation
RF	:	Radio Frequency
SNR	:	Signal to Noise Ratio
TIA	:	Transimpedance Amplifier
VLC	:	Visible Light Communications



LIST OF APPENDICES

Appendix A: VLC system room parameters MATLAB simulation coding	45
Appendix B: MATLAB coding to calculate the LOS channel gain.	47



CHAPTER 1

INTRODUCTION



1.1 Background

Light has widely been used for illumination since the start of civilisation, progressing from the simple usage of fire to more modern technologies such as conventional incandescent and fluorescent bulbs. Light has also been utilised to convey information and provide lighting, as humans can communicate over short and long distances through natural resources throughout history. With the invention of the photophone, a device that transmits a spoken signal on a beam of light, Alexander Graham Bell established the concept of using light as a communication medium in 1880. Bell focused sunlight with a mirror, then spoke through a machine that vibrated the mirror. The detector on the receiving end detected the vibrating beam subsequently decrypted it to recover the voice signal. Bell's experiment, however, was a disappointment since he was unable to establish a viable carrier frequency. Bell's studies were hampered by

sunlight, mist, and rain, so he halted them. The advent of the LED in 1927 revived the concept of visible-light communication that employs white light-emitting diodes to transmit information by flashing light at speeds that are unseen to human eyes. Visible-light communication has the advantage of being able to be utilised everywhere without distortion and providing high-speed communication. LED is utilised as the transmitter, and the photodiode or phototransistor is employed as the detector in visible-light communication. The transmission medium is the visible light spectrum as show in Figure 1.

The first viable white LED was created several years later, around 1996, using blue emitters coated with a yellow layer due to the advent of the blue LED [1][2][3]. LEDs have the added potential for encoding data onto light beams in addition to providing illumination. This permitted the development of optical wireless communications (OWC) as well as its sub-disciplines visible light communications (VLC) and free-space optical (FSO) communications [4][5].

Visible Light Communication (VLC) is a revolutionary innovation integrating data transfer and light-emitting diode (LED) illumination. VLC systems have the ability to provide high-speed wireless communications while also offering numerous advantages, including a large license-free bandwidth, low-cost components, strong encryption, and resilience to electromagnetic disturbance. Visible light communications (VLC) are used for high-speed, cable-free communication. Visible-light communication does not interfere with RF communications is a huge advantage. This allowed hospitals and space stations to use visible-light communication. Visible-light communication is becoming more popular for various applications due to its security, ease of implementation, and license-free band features.

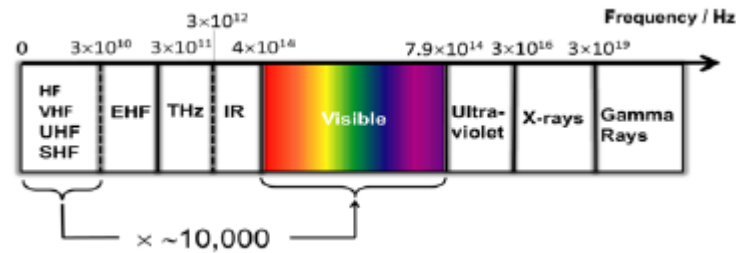


Figure 1: Frequency spectrum of the visible light spectrum in electromagnetic [6]

As intensive research has been done regarding the LED-based wireless VLC system, because of their excellent quality, excellent energy efficiency, and longer life lifetime, light-emitting diodes (LEDs) are progressively taking over conventional fluorescent light as illumination sources. Furthermore, a modulated driving signal can be superimposed on the direct current (DC) bias, the intensity of their generated light can be controlled, allowing for data transfer (AC component) and illumination (DC component) at the same time. As a result, LEDs offer an ideal solution as data transmission in interior contexts [4, 5]. LEDs are a suitable component for the VLC system as data transmitters for the indoor environment. Nonetheless, the study shows that the LEDs employed in the system have poor modulation bandwidths, restricting the data rate achieved. There have been reports of new advanced multilevel modulation formats, demonstrating that the next optical communication system can be solved in a variety of ways [6]. However, it appears that almost all of these advanced modulation forms require complex and expensive transmission methods. Advanced modulation formats that lower the system complexity while simultaneously attaining better bit rates and spectrum efficiency with fewer optoelectronic components will make the optical transmission system more viable and efficient. As a result, the carrier-less amplitude phase (CAP) modulation scheme is a promising

candidate for constructing a versatile, less complex, and cost-effective optical access as well as in network communications network. Aside from that, due to their low peak-to-average power ratio (PAPR) and straightforward transceiver design, this technology is appropriate for VLC systems. CAP modulation is just a multidimensional and multilevel modulation system that mimics quadrature amplitude modulation (QAM) at the phase in which it transmits two input data streams simultaneously. Because the working concept of CAP modulation is similar to that of QAM, it does not need local oscillators (LOs), RF mixers, or phase-locked loops, which unnecessarily complicate the electronic circuits. On the other hand, instead of using the carrier, CAP employs transversal filters with an orthogonal impulse response to produce in-phase and quadrature filters to segregate the data streams.

1.2 Problem Statement

Visible light communication (VLC) represents a promising new technology owing to the increasing proliferation of communication services. The main component of this technology is LEDs. However, with various LEDs available in the market, how do we determine the ideal LED? Other than that, although LED is an ideal candidate to be used as data transmitters in indoor environments. LEDs, on the other hand, which are commonly used in VLC, the modulation bandwidths are low, limiting the data rate that may be achieved. Carrier-less amplitude and phase (CAP) modulation have been recommended for the VLC system to boost possible data speeds. Nevertheless, among various modulation techniques that have been widely investigated to improve the VLC system's performance, is the CAP modulation suitable for the VLC system?

1.3 Objective of the project

The objectives of the project are to:

1. Simulate carrier-less amplitude phase (CAP) modulation for the VLC system.
2. Evaluate the carrier-less amplitude phase (CAP) performance within the VLC system.
3. Propose the suitability of CAP modulation system for indoor VLC system which use LED as an optical source.

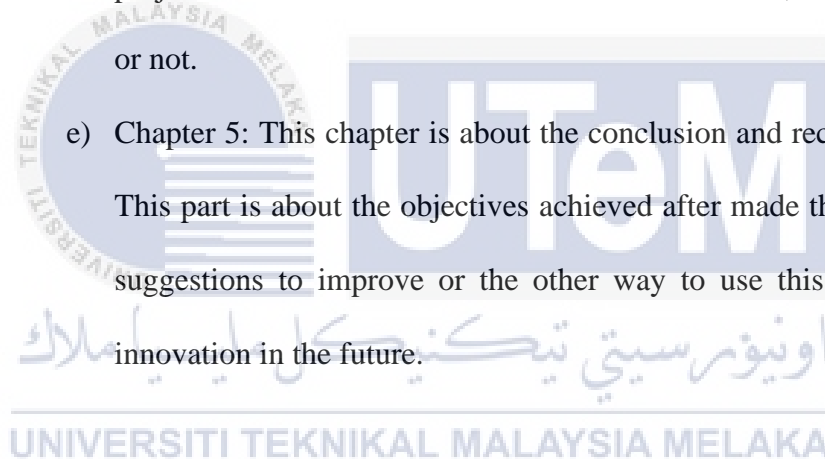
1.4 Scope of the Project

There are a few main scopes of work in this project. First, a basic VLC system is simulated using On-Off Keying (OOK) modulation in MATLAB. This is because OOK is the basic modulation system used in the VLC system. The criteria to focus on in this project are BER, eye diagram, and output power. Next, a suitable CAP modulation will be chosen. CAP modulation has a variety of modulation; nevertheless, m-CAP is chosen. Then, m-CAP modulation is simulated in the VLC system by changing the modulator of the OOK circuit constructed to Simulink. After that, the system's performance using CAP modulation is evaluated by comparing the result of CAP modulation to OOK modulation. Finally, CAP modulation will be proposed if it is suitable for an indoor VLC system.

1.5 Thesis Outline

This thesis contains five chapters to explain the development of the project Performance Evaluation of Carrier-less Amplitude Phase Modulation Scheme for Indoor Visible Light Communication (VLC) System are:

- a) Chapter 1: This chapter introduces the whole project. The basic and initial explanation will be discussed in this chapter. The introduction has discussed the project's background, project objective, problem statement and scope of the project.
- b) Chapter 2: This chapter contains the literature review about the theoretical concept of the applicant in this project.
- c) Chapter 3: This chapter is about research methodology that explains the steps that be used in this project.
- d) Chapter 4: This chapter focuses on the result and discussion of the project. The whole discussion is based on the result, either successful or not.
- e) Chapter 5: This chapter is about the conclusion and recommendation. This part is about the objectives achieved after made the projects and suggestions to improve or the other way to use this project or do innovation in the future.



CHAPTER 2

LITERATURE REVIEW



2.1 Introduction

The demand for a data communication network which can supply higher bandwidth at high-speed access grew day by day as the communication industry evolved. The solution could be a visible light communication (VLC) system, which has the ability to provide high-speed wireless communications with various advantages.

2.2 Visible Light Communication

Visible Light Communication (VLC) is a viable technology that integrates data transfer and light-emitting diode (LED) illumination. The LED serves as the transmitter in this communication system, and the photodiodes serve as the receiver.

A VLC system is depicted as a block diagram in Figure 2.

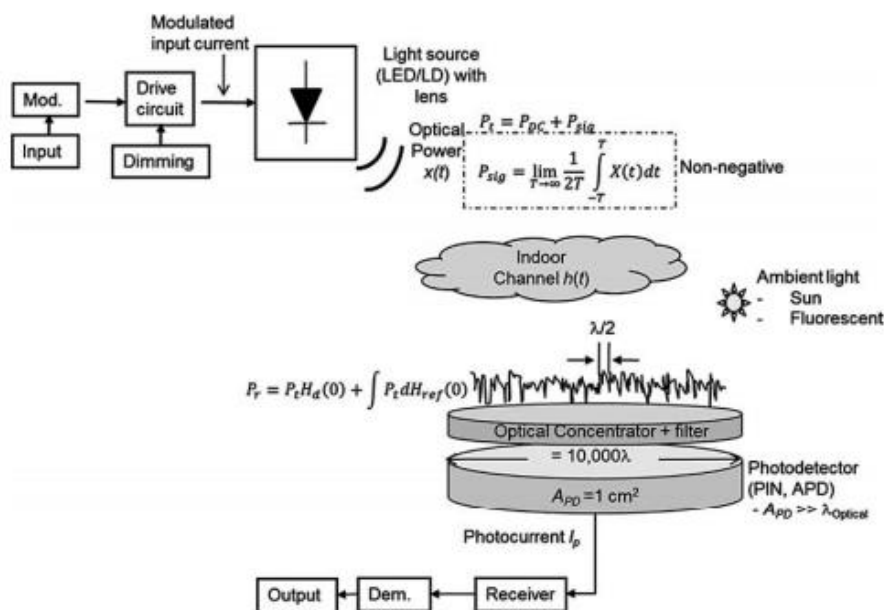


Figure 2: Block diagram of a VLC system.[1]

2.2.1 Comparison of RF-based links and VLC technology

Along with the increased usage of smart phones and the rise of the Internet of Things (IoT), the ever-increasing traffic on wireless networks has created a huge requirement for dependable high-speed data connections. Cisco predicts that by 2021, data traffic demand would have surpassed the 49 EB/month barrier, implying a 47 % annual increase from 2016, a sevenfold increase over 2016. (web, data and voice over IP 24%, video 54%, audio 37%, file sharing 49%) [6]. The Cisco VNI Global Mobile Data Traffic Forecast is listed in Table 1. Only cellular traffic is included in this projection, which eliminates traffic offloaded upon Wi-Fi and tiny cells from dual-mode devices. Readers, handheld gaming consoles, and other portable gadgets with inbuilt cellular connectivity fall into the "other portable devices" category. The "M2M" category includes wearables [6].

Table 1: Global Mobile Data Traffic, 2016–2021[6]

	2016	2017	2018	2019	2020	2021	CAGR 2016–2021
By Application Category (TB per Month)							
Web, data, and VoIP	2,153,676	2,938,884	3,779,988	4,674,801	5,538,615	6,434,681	24%
Video	4,375,000	7,225,123	11,415,329	17,564,661	26,067,686	38,148,326	54%
Audio streaming	559,999	843,394	1,193,711	1,620,662	2,103,876	2,674,183	37%
File sharing	151,874	258,617	403,273	592,352	820,954	1,102,867	49%
	2016	2017	2018	2019	2020	2021	CAGR 2016–2021
By Device Type (TB per Month)							
Nonsmartphones	109,505	137,852	169,955	199,173	236,257	269,189	20%
Smartphones	5,887,078	9,328,403	14,076,023	20,710,278	29,484,004	42,017,358	48%
Tablets and PCs	1,085,059	1,514,749	2,040,640	2,681,672	3,457,800	4,439,720	33%
M2M	157,998	284,415	505,292	861,025	1,409,949	2,224,543	70%
Other portable devices	910	599	391	328	432	659	-6%
By Region (TB per Month)							
North America	1,411,021	2,000,301	2,776,564	3,753,177	4,838,494	6,397,092	35%
Western Europe	736,377	1,084,396	1,534,120	2,167,831	3,019,843	4,189,615	42%
Asia Pacific	3,109,117	4,900,007	7,434,743	11,048,030	15,911,056	22,845,908	49%
Latin America	449,944	688,890	1,023,408	1,475,498	2,078,670	2,898,651	45%
Central and Eastern Europe	923,803	1,396,079	2,013,989	2,836,076	3,886,561	5,252,334	42%
Middle East and Africa	610,286	1,196,346	2,009,476	3,171,864	4,853,817	7,367,869	65%
Total (TB per Month)							
Total Mobile Data Traffic	7,240,550	11,266,018	16,792,300	24,452,476	34,588,442	48,951,469	47%

Present RF technology is having difficulty dealing with such increased data volume, resulting in spectrum congestion. VLC could be used as an alternative means of communication to help alleviate the current spectrum congestion which RF-based communication networks are experiencing, allowing for the development of high-data communication infrastructure as an alternative to traditional spectrum-limited and expensive RF-based wireless communication network [7]–[9]. Table 2 summarises various vital metrics that can be used to compare standard RF-based communication systems to VLC systems. VLC systems have an inherent security advantage over RF-based networks since the light beam is contained and thus cannot travel through the surrounding environment's barriers. In contrast to RF-based communications, whereby the radiation pattern is impossible to constrain within the antenna size. Another essential characteristic of VLC-based connections is the ability to regulate

and focus the light beam using lens and diffractive components, increasing the received power in the Rx. VLC also has the ability to produce low-interference communications due to the absence of RF interference in the light beam.

The benefits mentioned above, as well as VLC systems' cost-effective, high-power efficiency, and compatibility with current facilities [1], have prompted a series of research studies on VLC systems within the scientific society over the last decade, as evidenced by the huge volume of research and development findings published [9] and the references therein. Both data transfers and lighting are accomplished in VLC using LED intensity modulation (IM) and photodetector(PD) direct detection (DD)[1].

Table 2: Comparison between RF-based link and VLC technology

Property	RF	VLC
Bandwidth	Limited, regulated and congested	Huge and unregulated ~400 THz
Infrastructure	Requires custom infrastructure (i.e., base station and terminal)	Can use the existing LEDs lighting infrastructure
Licensing	Licensed and expensive	Free (i.e., Unlicensed)
Signal confinement	Can penetrate the walls	Cannot penetrate the walls (i.e., inherent security advantage)
Provided service	Communications	Illumination + communications
Noise source	Electrical and electronic components	Ambient light and sunlight
Mobility	Good	Limited
Radiation pattern control	Difficult to restrict antenna size	High ability of control when using lenses and diffractive elements

2.2.2 VLC's potential

The following are several interesting points that illustrate the potential of VLC[1]:

- LEDs are utilised in automobiles, buses, aeroplanes, trams, traffic lights, etc. White LEDs are also gradually yet steadily displacing ineffective fluorescent light in houses, workplaces, and perhaps street lighting. With the availability and affordability of high-brightness SSL gadgets increasing, this tendency will continue. (VLC is a technology benefiting from the emergence of SSL, the concept of generating light through solid-state electroluminescence.)
- Offered in low-cost transmitters and receivers, which include multi-array/element.
- Both SSL and VLC can take advantage of pre-existing (local) power lines including lighting infrastructure in workplaces, residences, and other locations. Thus, the last meter access network concept will become a reality by adopting hybrid power line communications (PLC) and VLC.
- VLC has no known health risks and does not interfere with present RF-based wireless networks. As a result, it is perfect for hospitals, aeroplane cabins, and other inherently safe places like petrochemical plants, nuclear power plants, mines, and so on.
- VLC inherent security is highly desirable in banking, retailing, manufacturing, healthcare, military, etc.
- Energy-efficient VLC is based on energy-efficient optical sources, LED in particular, and VLC is switched off when the light is turned off.

2.2.3 VLC's drawbacks

While there are numerous benefits to using a VLC system, however, there are a number of disadvantages. One of the most significant drawbacks is that it will only function in settings with electronic lighting. Traditional Wi-Fi can function at a reasonable distance from a residence, giving access to the internet while outside. Owing to the need for a lighting system, a VLC system would not be able to accomplish this. As a result, it will usually operate best in limited places where it is simple to guarantee that the room is well-lit.

The issue of obscuring the light needed to receive the signals is another downside of VLC systems. It would be simple to mistakenly disable the system's receiver. This might lead the signal to be disrupted, which may be caused by something as simple as a person walking through the room. Although this disadvantage might be addressed by using numerous light sources, it would still be simple to break the connection by mistakenly blocking the light sources.

Other potential issues would be mainly encountered with outdoor systems, such as the traffic signal system. Depending on the weather outdoors, there could be various problems with the system's operation. On gloomy days, it might work, but on sunny days, it is unlikely. During days when it is raining, snowing, as well as hazy, the signal may not be strong enough to be used. This problem can occur even in systems with a large number of windows.

2.3 Modulation schemes for VLC

The capacity of any digital communication system was derived by Shannon, as shown in the equation below.

$$C = B \log_2 \left(1 + \frac{S}{n} \right) \quad (2.1)$$

Where C represents the channel's capacity in bits per second, B represents the available bandwidth in Hz, S represents the signal power, and N represents the noise power. The equation above clearly shows that the communication system should have either very high bandwidth or high SNR to achieve a high data rate. Light received at a VLC receiver has gone through the free space optical channel, resulting in various losses, including received optical power per area, multipath reflections and interference from other light sources. This results in signal quality degradation and thereby reduction of SNR. It is not possible to increase the signal power of the VLC system without compromising eye safety or damaging the LEDs. All these factors contribute to a VLC system's available transmit power being limited.

Similarly, the modulation bandwidth of LEDs and other components limits the possible bandwidth of a VLC system. Any communication system has to utilise the available bandwidth efficiently for maximising data throughput. Modulation is the process of altering the characteristic of a carrier signal (a sinusoid) with the information to be transmitted. In RF communication, the properties of the carrier signal such as amplitude, phase, frequency or a combination of these are varied according to the information to be transmitted.

2.3.1 On-off keying (OOK)

OOK is a digital modulation method that is relatively basic. In this scheme, the incoming binary data stream is used to control the intensity of the LED by turning it ON to represent a binary one or turning it OFF to represent a binary zero. The OOK signal amplitude must be positive because the intensity modulation and direct detection (IM/DD) approach must be utilised, which is implemented as uni-polar non-

return-to-zero (NRZ) signalling. Each transmission symbol corresponds to a bit, and therefore the symbol rate corresponds to the bit rate. Due to its relative simplicity, OOK was adopted for optical wireless communication (OWC) early [10] in its modern history and widely [11]–[14]. The LEDs must be turned ON and OFF at faster rates to achieve higher data rates. An ideal OOK modulated signal has pulse shapes, as shown in Figure 3 with fast rise and fall times.

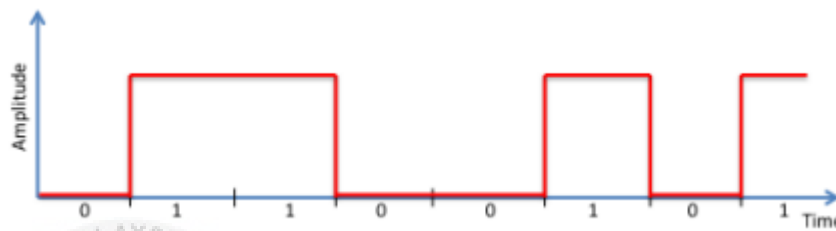


Figure 3: OOK modulation

The rise/fall times indicate the bandwidth required for a square pulse. The widely used rule of thumb relates the bandwidth and rise time of the square pulse, as shown below.

$$BW = \frac{0.35}{\tau_r} \quad (2.2)$$

Where BW is the bandwidth required for generating a square pulse with a rise time of τ_r (assuming rise time equal to fall time). The modulation bandwidth is determined by the lifetime of the minority carriers in the active area of the LEDs. The rise time is relatively constant, whereas the fall time depends on the voltage applied across the LED [15]. Dependence of rising and fall times on the internal parasitic capacitances (diffusion and junction capacitance) and their voltage dependence limits the modulation bandwidth and thereby OOK performance. Techniques such as carrier flush out [16] to remove the remaining carriers during the OFF phase and the resultant

faster fall times have caused an improvement in modulation bandwidth. However, due to the spectral inefficiency of the OOK scheme, it is not suited for high data rate systems.

2.3.2 Carrier-Less Amplitude Phase (CAP) Modulation

The CAP modulation technique has been extensively studied for VLC applications. This is owing to a unique mix of excellent spectral efficiency and ease of implementation [17]. Due to its unique qualities that contribute to implementation benefits in optical wireless communication (OWC), CAP modulation is currently frequently employed in VLC. CAP, being a single carrier modulation, offers a lower peak-to-average power ratio (PAPR) compared with discrete multitone (DMT), which one of the significant difficulties is high PAPR [18]. Due to the significant optical power constraints imposed by eye safety standards and design considerations on the transmitter front-end, the low PAPR factor of CAP modulation is ideally matched to OWC [18].

Furthermore, considering LEDs are incoherent light sources, designing an effective, coherent receiver is difficult. VLC incorporates the intensity modulation and direct detection (IM/DD) technology as a possible transceiver option [19]. Since the optical emitter's intensity is modulated in VLC, the data-carrying signal has to be real-valued, unipolar, and non-negative. Consequently, the CAP signal is real-valued, obviating the need for additional processing techniques like DMT's Hermitian symmetry [20]. In contrast to the quadrature amplitude modulation (QAM) equivalent, the CAP transceiver is comparatively easy to design since it utilises a digital finite impulse

response (FIR) filter and bypasses the requirement for carrier modulation and recovery [17].

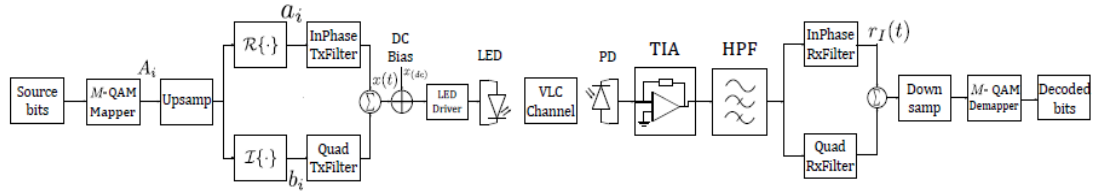


Figure 4: CAP transmission system's basic architecture [21]

Figure 4 depicts the CAP transmission system's basic architecture. The M-QAM mapper divides the stream of entering bits into b bit blocks and maps each block into one of $M = 2^b$ distinct complex symbols. Each complex symbol in the mapper outputs can be expressed with $A_i = a_i + jb_i$, whereby a_i and b_i denote the i th symbol's real and imaginary components, correspondingly. The mapper's outcomes are appropriately amplified to meet the total sampling frequency, f_s process. The in-phase (a_i) and quadrature (b_i) components are then supplied into the in-phase ($p(t)$) and quadrature ($\tilde{p}(t)$) digital pulse-shaping filters. The products of a root raised cosine filter (RRC) with a cosine and a sine function $p(t)$ and $\tilde{p}(t)$, are achieved correspondingly. These filters are orthogonal to one another, forming a Hilbert pair with the same amplitude response yet without 90° phase difference[22]. The filters' outputs are then added together with an appropriate DC bias to render it non-negative. The LED's intensity is modulated by the resultant signal, which is then transmitted across the VLC channel.

The radiated optical signal, $s(t)$, can be written as:

$$S(t) = \beta(x(t) + x_{dc}) \quad (2.3)$$

Where β is the electrical-to-optical conversion coefficient, x_{dc} is the DC bias, and $x(t)$ is the electrical CAP signal that is transmitted, which may be expressed as:

$$x(t) = \sum_{i=-\infty}^{\infty} [a_i p(t - iT) - b_i \tilde{p}(t - iT)] \quad (2.4)$$

The pulse-shaping filters are defined as follows:

$$p(t) = g(t) \cos(\omega_c t) \text{ and } \tilde{p}(t) = g(t) \sin(\omega_c t) \quad (2.5)$$

where $g(t)$ is the RRC, $\omega_c = 2\pi f_c$ is the centre frequency of the CAP signal, and T is the symbol duration.

At the receiver, a photodetector (PD) recovers the transmitted signal $x(t)$ from incoming optical radiation and converts it to a voltage signal using a trans-impedance amplifier (TIA). A high pass filter suppresses the DC component of the reconstructed electrical signal (HPF).

The transmitted pulse-shaping filters are then handed to the matched filters, which are conjugated, time-reversed counterparts of transmit pulse-shaping filters. The receiver estimates of the broadcast symbols are obtained by passing the output of the matched filters through the M-QAM de-mapper. Even with DC component excluded, the incoming electrical signal can be expressed as:

$$y(t) = \mathcal{R}P_t h(t) \otimes x(t) + w(t) \quad (2.6)$$

Where \mathcal{R} is the responsivity of the PD, P_t is the total transmit power, $h(t)$ is the channel attenuation and " \otimes " symbol denotes convolution. The $w(t)$ represents the ambient and thermal noise, modelled as additive white Gaussian noise (AWGN) with a mean of zero and double-sided spectral density of $N_0/2$. [10]

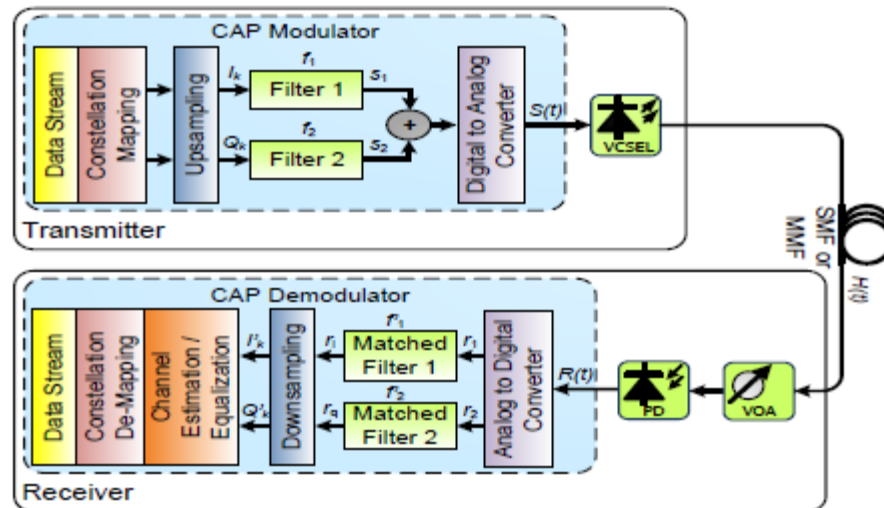


Figure 5: Basic CAP systems

As VLC system research continues to grow, various CAP variations were developed and demonstrated in recent years, as well as various multiplexing approaches. Various CAP modulation is listed as below:

1. Multi-band Carrier-less amplitude and phase

Multi-band CAP, also known as m-CAP. It was used as a multiband modulation method by arranging CAP signals on multiple subbands. The bandwidth of the network is divided into various frequency passbands. CAP-based signal transmission is accomplished on each of them using orthogonal pulse shaping filters, similar to traditional CAP, but with unique passband carrier frequencies f_{cn} , where the carrier frequency formula is and N is the number of used subbands. Compared to single-band CAP, the critical value of m-CAP would be its improved channel impairment tolerance. When m-CAP is communicated via a frequency selective channel, an estimation of flat frequency response could be attained in sub-band by differentiating the single wideband CAP into numerous small sub-bands. It also avoids the possibility of producing wideband filters, resulting in better bit error rate (BER) performance.

However, because the usage of N sub-bands necessitates N times the amount of electronic components (FIR filters, equalisers) than the traditional (single band) CAP approach, the system's implementation complexity skyrockets. Additionally, multiband CAP generates a modulating signal with a higher PAPR than single-carrier CAP, making it more vulnerable to nonlinear transmission defects.

2. Multiple-input multiple-output techniques

MIMO techniques are proposed to be combined with CAP-based transmission in VLC networks, and an experiment with a 44 imaging MIMO system and m-CAP modulation is conducted [23], [24]. This approach enables the transmission of higher aggregate data rates over the VLC channel. To ensure optimal performance, however, separate channel gains are required for different VLC links. As a result, these strategies are not appropriate for inside situations, as that is not always the situation in certain indoor places.

3. Spatial carrier-less amplitude and phase

S-CAP is offered a way of increasing the spectral efficiency of CAP yet keeping its simplicity. S-CAP takes advantage of extra information bits encoded upon the transmitting LED's position (or index). An additional $\log_2(N_t)$ data bit is stored on the index of the transmitting LED. Hence, the S-CAP achieves better throughput than the ordinary CAP by transferring additional bits in the spatial domain. The advantages of the S-CAP are that it consumes less bandwidth than CAP for a fixed number of transmitted bits/symbols and sends more bits/symbols for a fixed bandwidth requirement, resulting in improved spectral efficiency.

Table 3a: Experiments demonstrating the transmission of data via CAP in VLC systems [37]

year	ref.	LED source			CAP modulation parameters	blue filter	equalization		multiplexing		aggregated data rate (Gb/s)	distance (m)
		#	Type	3 dB BW (MHz)			pre-	post-	WDM	MIMO		
2017	[84]	1	white		CAP-128							1
												→ experimental study on proposed synchronization method (CAP-filter)
2017	[101]	1	red		m-CAP, 5 subbands, 16-QAM		Yes	Yes			0.32	
												→ demonstration of the use of a machine-learning algorithm to improve the performance of post-equalization
2017	[58]	1	white	1.2	m-CAP, m: {2,4,6,8,10}, up to 256-QAM						0.012	1
												→ optimization of filter parameters for m-CAP transmission
2017	[129]	1	red		FTN-CAP, 1/2 subbands, 4- & 16-QAM			Yes	Yes		1.47	1.5
												→ demonstration of FTN pre-coding in a CAP-based VLC link
2018	[130]	1	red		FTN-CAP, CAP-4			Yes	Yes		1.01	1.5
												→ demonstration of the use of look up tables to implement pre-coding in FTN-CAP
2018	[111]	4	white	1.9	m-CAP, 20 subbands		Yes		Yes		0.249	1
												→ experimental demonstration of use of m-CAP and MIMO to improve the aggregate data rate
2018	[123]	1	blue	10.8	SI-CAP, 4 subbands, 3 active, 4-QAM			Yes			1.032	1
												→ demonstration of the subband index (SI-) CAP scheme
2018	[124]	1	white	1.2	SN-CAP, 2/10 subbands, 4-QAM						0.004	2
												→ demonstration of super-Nyquist (SN-) CAP scheme
2018	[96]	1	red		SN-CAP, 2 subbands, 16-QAM		Yes	Yes			1.26	1
												→ demonstration of improved performance using super-Nyquist (SN) CAP
2018	[59]	1	white		CAP-4, CAP-16						0.009	0.1
												→ experimental study on the performance of CAP-based transmission using modified (Xia and BTN) pulse shapes

Table 3b: Experiments demonstrating the transmission of data via CAP in VLC systems (continue) [37]

year	ref.	LED source			CAP modulation parameters	blue filter	equalization		multiplexing		aggregated data rate (Gb/s)	distance (m)	
		#	Type	3 dB BW (MHz)			pre-	post-	WDM	MIMO			
2018	[116]	1	white	5	m-CAP, 10 subbands, 256-QAM								
					→ demonstration of the use of Xia pulses in a CAP-based VLC link								
2018	[61]	1	white	6.5	CAP-16				Yes		0.08	1	
					→ demonstration of the use of fractional-spaced FFE post-equalizer in a CAP-based VLC link								
2018	[100]	1	red		m-CAP, 5 subbands, 16-QAM		Yes	Yes			0.32	0.75	
					→ demonstration of the use of pre-distortion schemes based on a machine learning algorithm								
2018	[68]	3	RGB		CAP-32, CAP-64, CAP-128		Yes	Yes	Yes		1.75	1	
					→ demonstration of high aggregate data transmission in a CAP-based VLC link								
2019	[125]	1	white	1	SN-CAP, 2 / 10 subbands, 4- & 16-QAM						0.01	2	
					→ experimental study on the performance of super-Nyquist CAP scheme								
2019	[29]	1	white	1.4	m-CAP, 20 subbands, up to 128-QAM		Yes	Yes			0.163	2.15	
					→ demonstration of a multi-user indoor VLC system based on m-CAP data transmission								
2019	[57]	1	red	6.5	CAP-16, CAP-32, CAP-64				Yes		0.2	15	
					→ demonstration of high-speed CAP-based data transmission over a VLC links using FPGAs (real-time system implementation)								
2019	[126,127]	1	red	0.5	SN-CAP, 4 subbands						0.006	0.05	
					→ proposal and demonstration of hybrid SN-CAP schemes (staggered CAP and hybrid SN-CAP)								
2019	[106]	1	white		CAP-64	Yes			Yes		2.4	1.1	
					→ use of a deep neural network as a post-equalizer to improve link performance in CAP-based transmission								

Table 3 below sums up various types of experimental demonstrations. The information in Table 3 is based on the source type and CAP-based modulation technique used, the connection distance, and the type of equalisation and multiplexing used. From Table 3, it can be observed that the previous research trend shows that to improve and attain an improvement in data rates and spectral efficiency using CAP modulation in the VLC system, additional complexity is introduced into the system. Examples of additional complexity introduced are using a more complex modulating signal or implementing more sophisticated equalisers. Although numerous experimental findings have been published, little theoretical research has been published [27].

Several computational studies and a few experimental investigations [26, 27] that directly evaluate the performance of an LED-based VLC connection when using CAP, PAM, and O-OFDM schemes [25, 28]. The authors of [27] indicate that the PAM and CAP schemes investigated are equivalent in performance and that O-OFDM produces the worse outcomes owing to the scheme's vulnerability to nonlinear distortions (greater PAPR). Likewise, in [28], the writer demonstrates that the CAP system performs marginally better than O-OFDM for the same link. Comprehensive correlation (both simulated and experimental) among these three basic modulation schemes have been conducted in the scenario of high-speed fibre-based optical connections, with an emphasis on link power margins, energy efficiency, and complexity [28]–[31]. While these links do not have the same attributes as optical wireless LED-based links (differences in the nonlinear behaviour of laser diodes and LEDs as well as dispersion of the link), several general observations about the performance evaluation of these modulation techniques can be made based on these results as shown in Table 4. Despite the fact that PAM has the lowest complexity and

highest energy efficiency, it is inefficient over long distances or at greater data rates when O-OFDM and CAP can be used as alternatives. While O-OFDM schemes are the most efficient in terms of spectral efficiency, yet high PAPR results in nonlinear impairments. CAP systems have been shown to achieve data speeds comparable to OFDM while being more energy efficient and presumably less complicated, enabling for hardware implementation. Researchers employed measures like the number of needed components and also the number of real-value multiplications to conduct an unbiased assessment of system complexity [29, 32–34]. The results reveal the single-carrier CAP utilizing low-order QAM modulation is simpler than OFDM methods. Higher-order or perhaps more sophisticated CAP modulation (including multi-band CAP) can, however, be as complex as O-OFDM. Likewise, equivalent experimental demonstrations and comparative analyses have already been conducted aimed at POF links based on LEDs and laser diodes [31,35,36,37]. Even though Table 4, summarises the relative merits of these three fundamental modulation schemes, the intrigued viewer should consult the cited articles for detailed comparisons for qualitative analysis, as the results are highly dependent on the type of link, the modulation order, and the component characteristics used. Lastly, it is worth noting that adding equalisation to the link to boost the possible data rates complicates the system [32]. Equalisers that are linear in nature (e.g. FFE and DFE) are pretty simple to implement, especially in the case of LED-based networks with low symbol rates (up to a few Gbaud). Nonlinear equalisers, on the contrary, necessitate a larger number of components or other form of digital signal processing that could not be achieved with simple hardware.

Table 4: A comparison of performance evaluation of the relative advantages of modern modulation formats [37].

Scheme	Spectral efficiency	Energy efficiency	Complexity
Single-carrier CAP	+	++	++
m-CAP/ CAP variants	++	+ / ++	+ / ++
PAM	+	+++	+++
O-OFDM	+++	+	+

2.4 Light Sources

To implement visible light communications, the light sources that emit the light must possess the following important properties: wavelength, linewidth, numerical aperture, excellent brightness with a small emitting surface area, long life, high reliability, and even a large modulation bandwidth [38]. LEDs and LDs are the most frequently utilised light sources as both of these light sources depend on the excitation state in semiconductor materials to work. LEDs and LDs have a unique property or advantage. They are compact and provide low forward voltage and driving current [39]. The human eye's visible range is 400nm to 700nm, and with LEDs/LDs, research is being conducted to generate light throughout a greater spectrum of wavelengths from visible to infrared [1]. To generate light in the LEDs/LDs, the transition of an electron in a semiconductor material should occur where the electron transitions from an excited state to a lower energy state. This electron transition, which arises due to the difference in the energy states, leads to the generation of two processes named the radiative process and the non-radiative process. The radiative process generates light,

and the non-radiative process leads to heat generation. "An electron in the lower energy state (conduction band) returns to the empty state in the valence band. It is a simultaneous process. It does not require any additional energy, and this process is named radioactive recombination. This process is associated with the functioning of the LEDs" [40].

2.4.1 Light Emitting Diode

The LED is a semiconductor device with a P-N junction. The optical radiation occurs whenever we subject it to an electronic excitation by placing a forward bias voltage across the p-n junction. This process energises the electrons in the material, causing them to reach a 'excited state,' which would be very unstable. When these electrons reach the excited state, they return to the stable state after some time, leading to the release of energy(photons). The passage of electrons from the valence band to the conduction band and back again from the conduction band to the valence band is what causes the LEDs to function. This process is called radiative recombination [40].

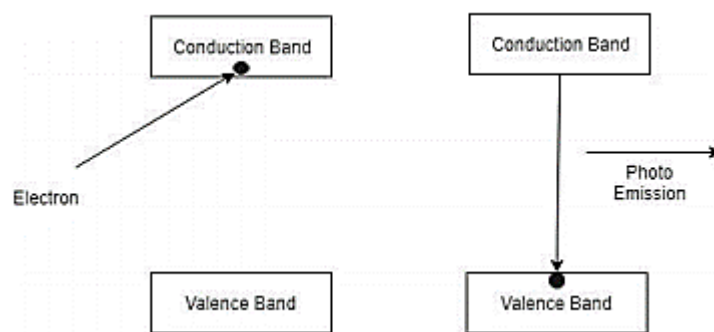


Figure 6: Functioning of Semiconductor Devices

From Figure 6, we can consider the conduction band as energy state E_2 and Valence band state is taken as E_1 the difference in these states results in Photon Emission. [40]

$$\text{Energy} = \text{Energy state } E_2 - \text{Energy state } E_1 = hf = \frac{hc}{\lambda} \quad (2.7)$$

Where E_2 and E_1 are the two energy levels, h denotes Planck's constant, f denotes frequency, c is the speed of light, and λ is the wavelength of absorbed or emitted light.


The selection of the LEDs depends upon three properties or factors: LED modulation band, luminous efficiency, and power efficiency.



CHAPTER 3

METHODOLOGY

3.1 Introduction



There are a few main scopes of work in this project. First, a basic VLC system is simulated using On-Off Keying (OOK) modulation in MATLAB. This is because OOK is the basic modulation system used in the VLC system. The criteria to focus on in this project are BER, eye diagram, and output power. Next, a suitable CAP modulation will be chosen. CAP modulation has a variety of modulation; nevertheless, m-CAP is chosen. Then, multiple-band CAP modulation is simulated for the VLC system by developing the system in MATLAB Simulink. After that, the system's performance using CAP modulation is evaluated by comparing the result of CAP modulation to OOK modulation. Finally, CAP modulation will be proposed if it is suitable for an indoor VLC system.

3.1.1 System Flow Chart

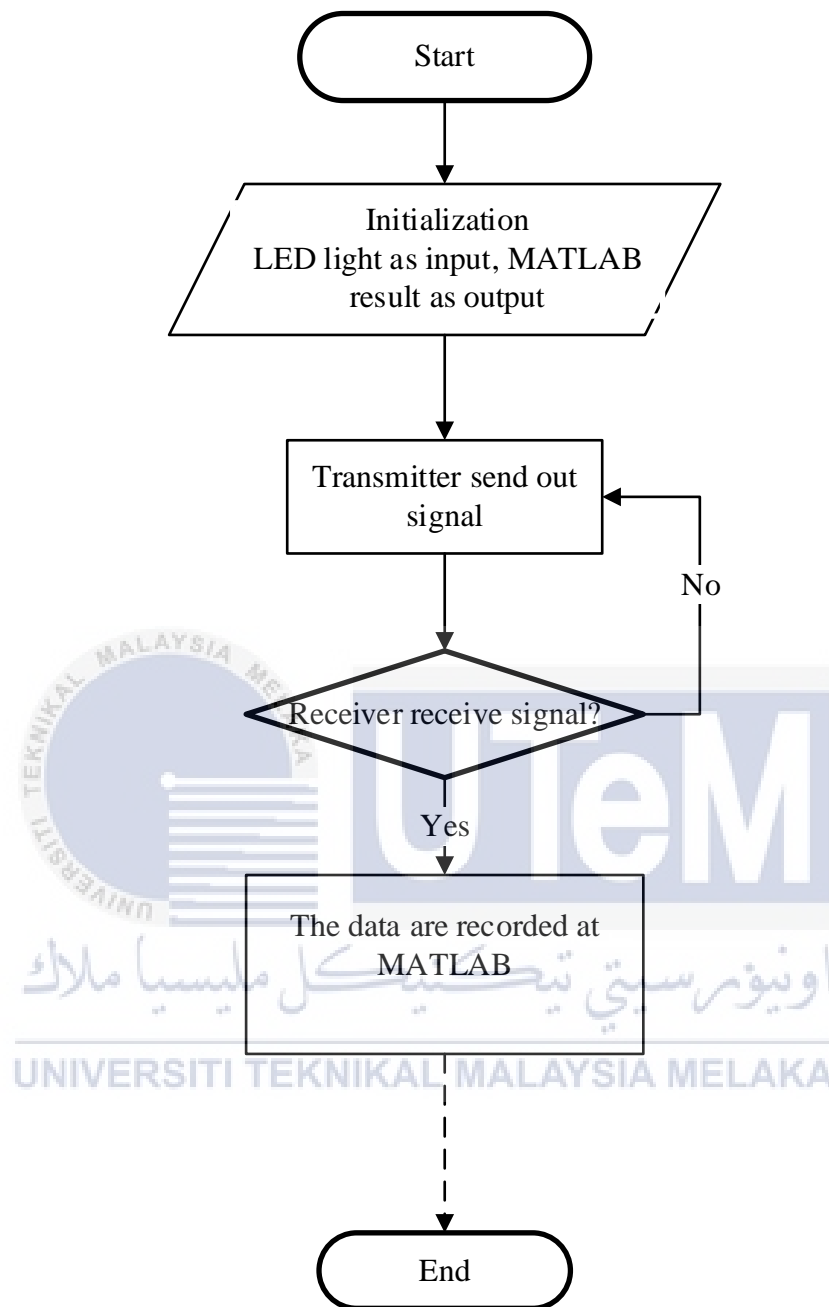


Figure 7: System flow chart

Figure 7 shows system's flow is when the LED transmitter sends out a signal, the photodetector, the receiver, will be run to determine if the signal is received. If the signal is received, the system will try to send out another signal, while if the signal is received, then the output will be recorded in MATLAB.

3.2 Implementation of the system parameters

This paper discussed an indoor VLC system comprised of a single transmitter and receiver. The system parameters are determined in Table 5, and the values will be used in MATLAB. Here the project is considering a single-LED array. After reviewing multiple IEEE papers and books, these parameters are considered [1][2][3]. To analyse VLC system performance, the parameter of a room, LED, receiver and noise are set. That parameter is listed in below Table 5. Table 5 summarises the critical factors for a typical room setting that are utilised in VLC system modelling.

Table 5: Main simulation Parameters

VLC Ideal Parameter		
Type	Parameter	Value
Transmitter	Number of Transmitters (LED)	1
	Power Radiated by LED	1W
	Angle of Irradiance	70
	Field of View (FOV)	70
	LED location in the room	[2,2,2]
	Number of LEDs per array	60*60
	Center Luminous Intensity	0.73
Room & Other	Size of Room [W x L x H]	[4 x 4 x 2] m
	Noise Current	0.562 A
	Amplifier Bandwidth Factor	50×10^6

	Ambient Light Power	5×10^{-12} A
	Data Rate	1×10^6 b/s
	Distance Between Tx and Rx	1m
	Filter Coefficient	1
	Electron Charge	1.6×10^{-19}
Receiver	Photodetector Area	1×10^{-4} cm ²
	Angle of Irradiance	70
	Field of View (FOV)	90
	Responsivity	1 A/W
	Photodetector Concentrator Refractive Index	1.46

The room's appropriate size is set to be 4 meters in length, 4 meters in width, and 2 meters in height. The LED is located in the room's centre [2,2,2]. Theta(θ) is the half-power semi-angle for the transmitter; it is defined as the angle formed between the wall and the placement of the LED, which is 70° .

The LED source transmits 1W of electricity, and the luminous intensity that the human eye can see is between 300-910lx [1]. The active area of the photodiode or the receiver is given as 1×10^{-4} cm². The half-angle FOV for the receiver is taken as 90° as it is the angle at which the reflections are considered. Therefore, it is considered to be constant.

3.3 VLC system coding

The following is the MATLAB simulation coding used for the project. The explanation of the coding is written next to code after '%' and is colour green for better understanding.

3.3.1 Room parameters simulation coding

```

% BASIC PARAMETER REQUIRED %

Incidence = 70*pi/180;

TX_FOV = 70;           % Transmitter Field Of View
RX_FOV = 90;           % Receivers Field Of View

Tx = [2,2,2];          % Transmitter Location
%Rxp = [2,2];          % Receiver Location

W_Room = 4;            % Width of Room
L_Room = 4;            % Length of Room
H_Room = 2;            % Height Between Transmitter and Receiver
R = 1;                 % Responsivity of Photodiode

Apd = 1e-4;            % Area of PhotoDetector
Rb = 1e6;              % Data rate of system

Iamp = 5e-12;          % Amplifier Current
q = 1.6e-19;           % Electron Charge
Bn = 50e6;             % Noise Bandwidth
I2 = 0.562;            % Noise Bandwidth Factor
PLED = 1;              % Power Emitted by LED

index = 1;
HLED = 1;

```

```

[W L] = meshgrid(-(W_Room/2) : 0.50 : (W_Room/2)); % Consider Length
of block for Room

xydist = sqrt((W).^2 + (L).^2);

hdist = sqrt(xydist.^2 + HLED.^2);

%D = Tx - Rx;

%d = norm(D);

%Incidence = acos()

A_Irradiance = ((Tx(3)-HLED)/hdist);

%I(index) = Irradiance*180/pi;

%if abs(Incidence <= RX_FOV)

    p = TX_FOV ;
    Tx_FOV = (TX_FOV*pi)/180;
    % BASIC CALCULATION IN VLC SYSTEM %
    % Lambertian Pattern
    m = real(-log(2)/log(cos(Tx_FOV)));
    % Radiation Intensity at particular point
    Ro = real(((m+1)/(2*pi)).*A_Irradiance^m);
    % Transmitted power By LED

    Ptx = PLED .* Ro;

    % Channel Gain ( Channel Coefficient Of LOS Channel )

    %Theta=atand(sqrt(sum((Tx-Rx).^2))/H_Room);

    HLOS = (Apd/hdist.^2).*cos(Incidence).*Ro;

    % Received Power By PhotoDetector

    Prx = HLOS.*Ptx;

    % Calculate Noise in System

```

```

Bs = Rb*I2;

Pn = Iamp/Rb;

Ptotal = Prx+Pn;

new_total = new_shot + new_amp;

SNRI = (R *Prx).^2./ new_total;

SNRdb = 10*log10(SNRI);

%     else

%         SNRI = 0;

%         SNRdb = 0;

%     end

index = index + 1;

% Plot Graph %

figure;

mesh(W,L,SNRdb);

%mesh(SNRdb);

%ylim([0 30]);

title('SNR Distribution in Room');

xlabel('Length of Room');

ylabel('Width of Room');

zlabel('SNR in dB');

```

3.3.2 Coding to calculate the LOS channel gain

```

theta=70; % semi-angle at half power

m=-log10(2)/log10(cosd(theta)); %Lambertian order of emission

P_total=1; %transmitted optical power by individual LED

Adet=1e-4; %detector physical area of a PD

%% Optics parameters

Ts=1; %gain of an optical filter; ignore if no filter is used

index=1; %refractive index of a lens at a PD; ignore if no lens is used

FOV=70*pi/180; %FOV of a receiver

G_Con=(index^2)/sin(FOV); %gain of an optical concentrator

%% Room dimension

lx=4; ly=4; lz=2; % room dimension in meter

h=2; %the distance between source and receiver plane

Nx=lx*20; Ny=ly*20; % number of grids in the receiver plane

XT=0; YT=0; % position of LED;
x=-lx/2:lx/Nx:lx/2;
y=-ly/2:ly/Ny:ly/2;

[XR,YR]=meshgrid(x,y); % receiver plane grid

D1=sqrt((XR-XT(1,1)).^2+(YR-YT(1,1)).^2+h^2);

% distance vector from source 1

cosphi_A1=h/D1; % angle vector

H_A1=(m+1)*Adet.*cosphi_A1.^(m+1)./(2*pi.*D1.^2);

P_rec_dBm=10*log10(P_rec);

meshc(x,y,P_rec_dBm);

```

```

xlabel('X (m)');
ylabel('Y (m)');
zlabel('Received power (dBm)');
axis([-lx/2 lx/2 -ly/2 ly/2 min(min(P_rec_dBm)) max(max(P_rec_dBm))]);

```

3.3.3 Illumination Distribution

```

theta=70; %semi-angle at half power
m=-log10(2)/log10(cosd(theta)); %Lambertian order of emission
I0=0.73; %Center luminous intensity total according to number of LEDs
I0_total=60*60*I0; % room dimension in metre
lx=4; ly=4; lz=2; %the distance between source and receiver plane
h=2; % position of LED
[XT,YT]=meshgrid(2,2);
Nx=lx*20; Ny=Ny;
x=linspace(0,lx,20); y=linspace(0,ly,20);
[XR,YR]=meshgrid(x,y);
Vector_Distance=sqrt((XR-XT(1,1)).^2+(YR-YT(1,1)).^2+h^2);
% distance vector from source
cos_phi=h./Vector_Distance;
% vector containing the angle of irradiance (of the LED) for each position
E_lux=(I0_total*cos_phi.^m)/(Vector_Distance.^2);
% LIGHT FLOW or LIGHTING (in lux)
meshc(x,y,E_lux);
xlabel('X (m)'); ylabel('Y (m)'); zlabel('Illuminance(lx)');

```

3.4 OOK Modulation

The following is the MATLAB simulation coding used for OOK modulation. The explanation of the coding is written next to code after '%' and is colour green for better understanding. For the OOK modulation, 100000 bits were set for SNR of 0 to 15db. An AWGN channel was utilised to introduce white Gaussian noise into the transmitter stream. The output of this code is the BER graph, scatter plot and eye diagram.

```

% Simulation of OOK-NRZ transmission with using Monte Carlo simulation

% Initialization

Po=1;

R=1;

Tbs=1;

M=1000000; % Frame length (x_1 x_2 ... x_M)

SNRdB=0:15; % SNR in dB

SNR=10.^(SNRdB/10);

Rate= zeros(1, length(SNRdB));

% Transmitter

for dB= 1: length(SNRdB) % start looping by SNRdB

%OOK-NRZ signal generation

x_inp=round(rand(1,M)); %

s=x_inp.*2*Po;

Es=2*Po^2*R^2*Tbs; % Es=Eb

sigma=sqrt(Es/(2*SNR(dB)));

```

```

% Channel

y_channel=awgn(s,SNRdB(dB));% Additive White Guassian Noise (AWGN)

y_channel=s+sigma.*randn(1,M);% Additive White Guassian Noise (AWGN)

x_out= round(y); %

% Bit Error Rate (BER) calculation

[err, rate]= symerr(x_inp, x_out);

Rate(dB)= Rate(dB) + rate;

end % end for loop

Rate(dB)= Rate(dB); %

% Plot the simulation result

f1 = figure(1);
set(f1,'color',[1 1 1]);
semilogy(SNRdB,Rate, 'b-*')
hold on;
xlabel('Signal-to-Noise Ratio (SNR)');
ylabel('Bit Error Rate (BER)');
title('Simulation OOK-NRZ transmission over noise');

legend('BER simulation')

grid on;

scatterplot(x_out);

eyediagram(x_out,M);

```

3.5 CAP modulation

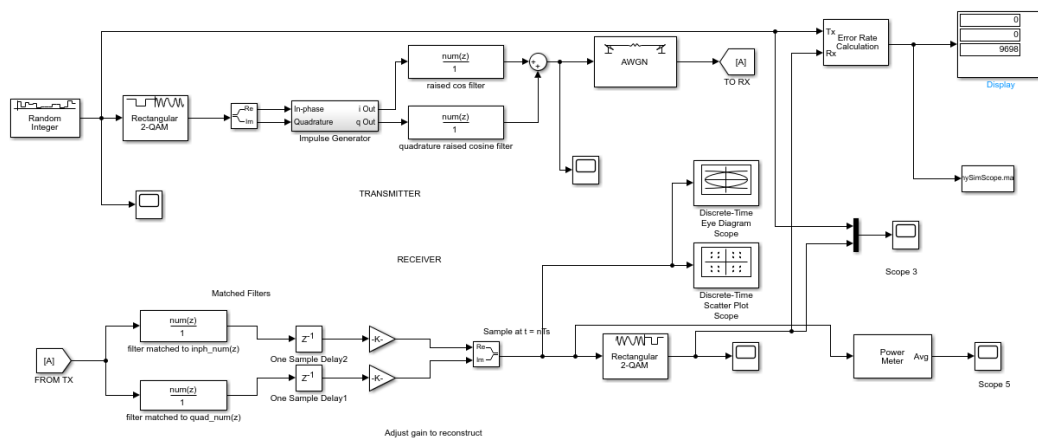


Figure 8: CAP-2 scheme

The standard CAP-2 scheme, depicted in Figure 8, was developed using MATLAB Simulink. This CAP was created using MATLAB Simulink's rectangular quadrature amplitude modulation module. As a result, generate CAP-2. The QAM is identical to the CAP in that it allows for multiple levels and modulation in several dimensions. Nevertheless, CAP does not generate two orthogonal components with a sinusoidal carrier. As a result, the ratio of sample-to-symbol is proportional to the dimension count in a linear way. Additionally, it also explains how the orthogonal waveform is generated using the CAP.

Both the transmitter and receiver use digital technology. The procedure is referred to as encoding in the transmitter section. The transmitter will decompose the data stream into blocks of binary data. A single pair is used to encode each data block. Two orthogonal signals are formed after encoding, which are then merged before transmission. For that implementation, the incoming sequences are up-sampled to match the implementation sampling rate, and hence the rate of this procedure. The AWGN channel with the 10 dB SNR level is set for modelling noise in this block.

In the meantime, the process is referred to as decoding at the receiver end, and it is responsible for decoding the data symbol in order to recover the block binary digits. The receiver's output is down-sampled to the original symbol rate. Separation of the two orthogonal summed modulated signals is possible.

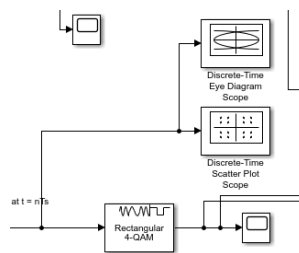


Figure 9: Eye diagram scope and scatter plot Connection

Next, when the program is run, the eye diagram scope and scatter plot are shown as a result. To observe the eye diagram and scatter plot, a Discrete-Time Eye Diagram scope block and Discrete-Time Scatter Plot block is connected to the port before Demodulator, as shown in Figure 9. To obtain a BER graph, the following MATLAB code is run. This is because the Error Rate Calculation block data are sent to a mat file. First, 'mySimScope' files are loaded into the workspace, then the coding to find BER is run. 'mySimScope' is the mat file name while 'SimScope' is the variable name for the To File block. As there are a few thousand data, only the first 10 data are taken from the workspace to plot the data.

```
load('mySimScope.mat')
EbN0=0:9;
% signal-to-noise ratio in dB.
SNR=10.^(EbN0./10);
% signal-to-noise ratio
Y = SimScope(2,1:10)
figure;
semilogy(EbN0,Y,'r-X','linewidth',2);
grid on
legend('simulation');
xlabel('Eb/No, dB');
ylabel('Bit Error Rate');
title('Bit error probability curve for CAP-2 modulation')
```

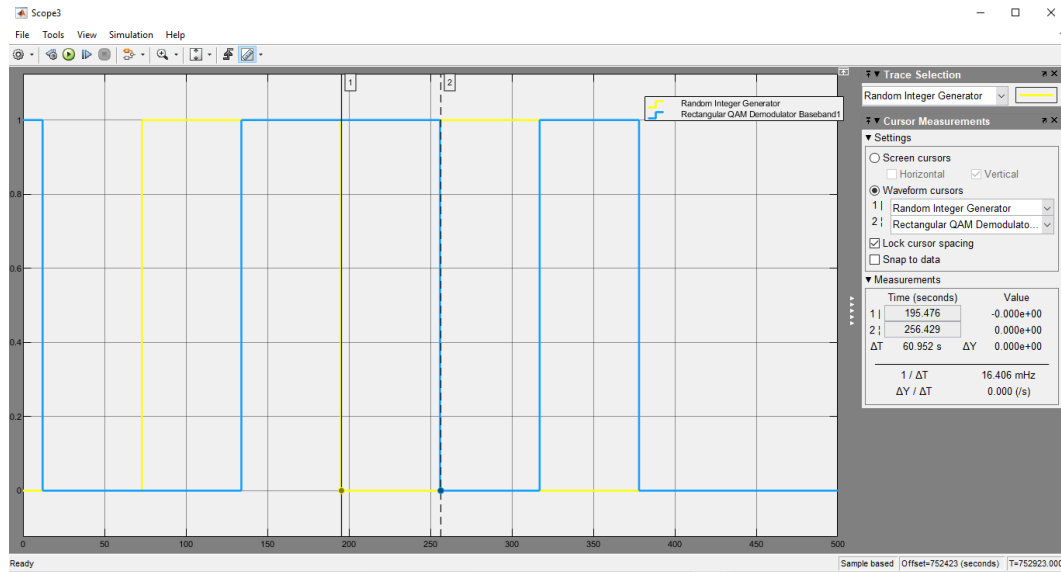


Figure 10: Transmitted and received pulse

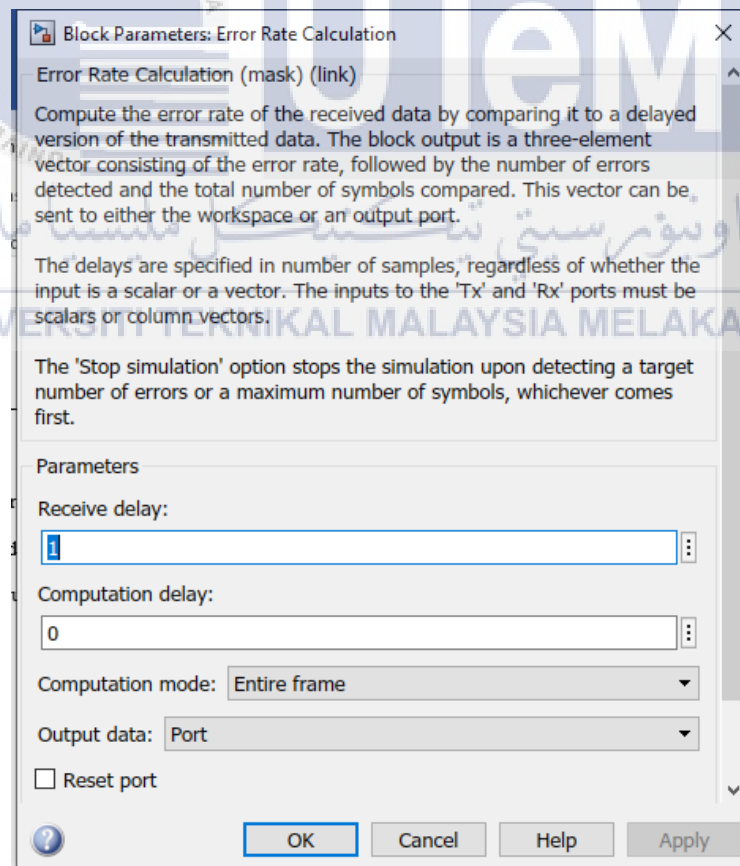


Figure 11: Error Rate Calculation block

Then, in scope three from Figure 10, it can be observed that there is an approximate 60 s delay in bit error rate between Random Integer Generator Block and Rectangular QAM Demodulator block. Therefore, to avoid error in Error Rate Calculation block, 1 min delay is set in Received Delay input parameter as shown in Figure 11.

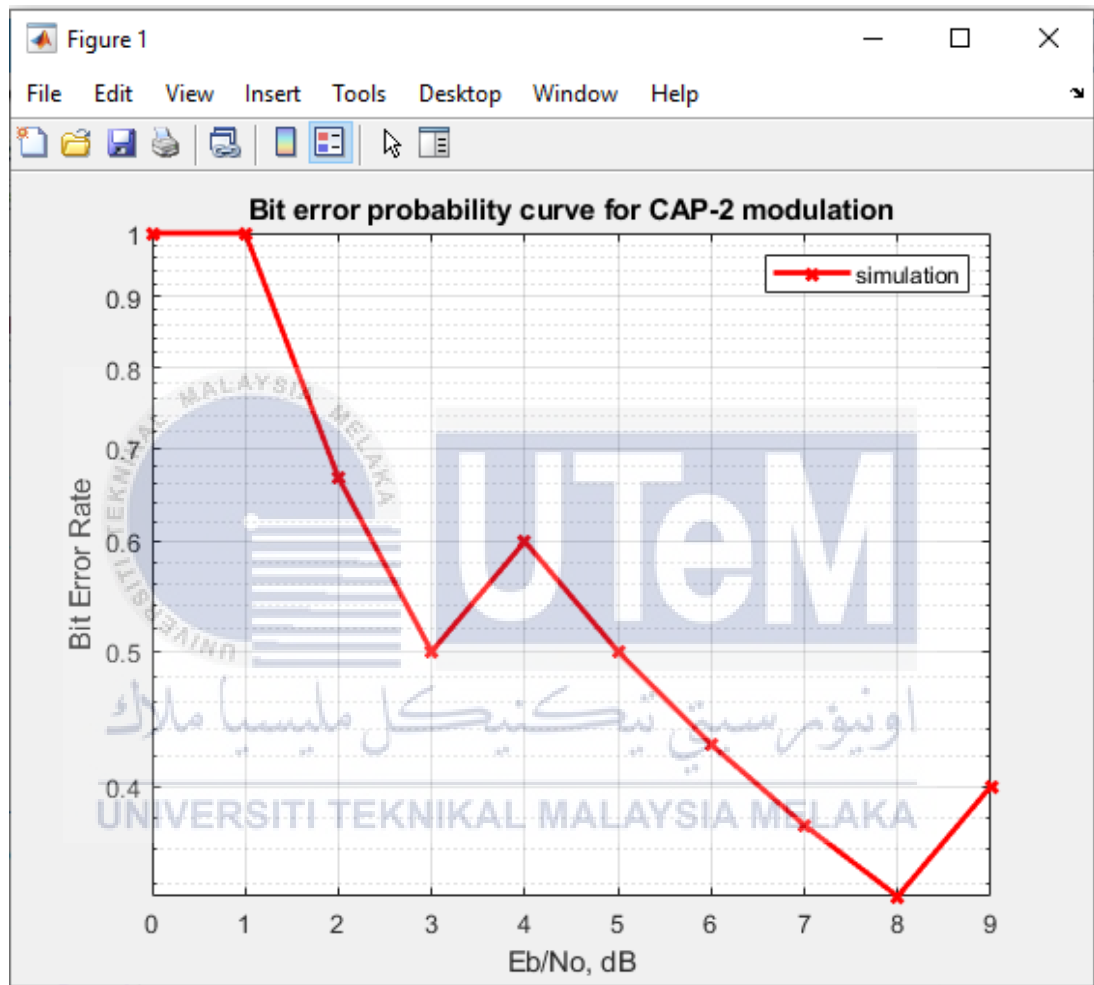


Figure 12: BER graph for CAP-2 without delay

Without the 1 min delay in the Received Delay input parameter, the BER graph will be shown in Figure 12. This is because input will be calculated as real-time data where if compared, the received data are actually 60s late due to a delay block use in the Simulink CAP modulation.

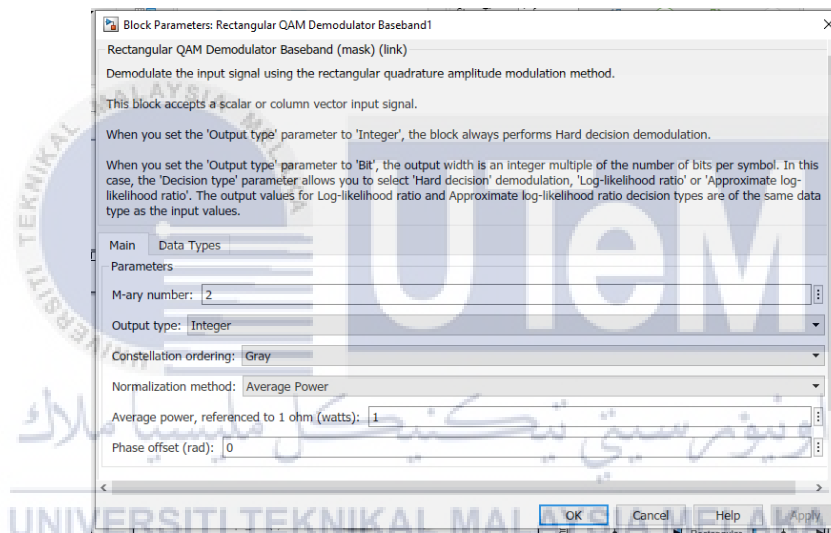
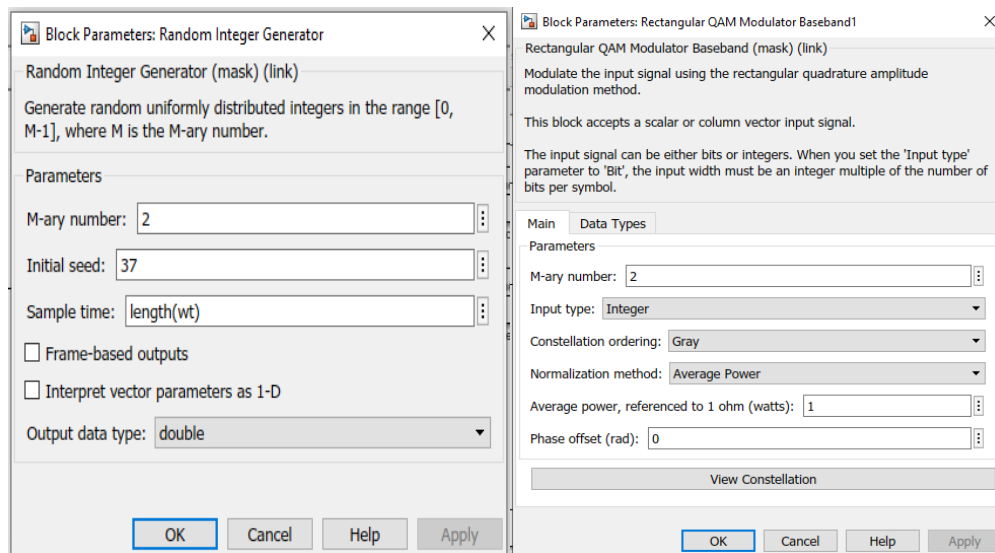


Figure 13: Block diagram for QAM modulation and demodulation and random integer generator

By changing the M-ary number at QAM modulation and demodulation block and random integer generator block, CAP-4 and CAP-8 can be simulated as shown in Figure 13. After changing the M-ary number in the block, the Simulink are run to obtain the BER graph, scatter plot and eye diagram. However, depending on the name of the 'To File' block, the coding name for the file name needs to change corresponding to obtain the BER graph.

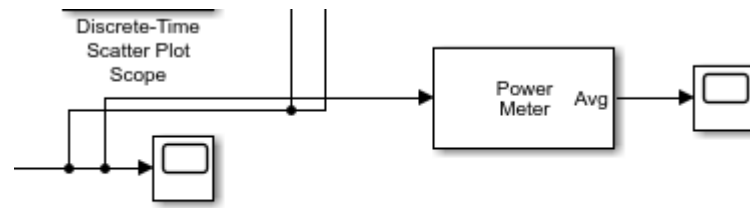


Figure 14: Power meter connection

To find the power received in dBW for CAP modulation, a Power Meter block is used. The Power Meter block is used to determine the power of a voltage signal. Average power, peak power, and peak-to-average power ratio are all included in the power measurements. The block computes these values using the sliding window approach. After the QAM demodulator, this block is connected to the port to observe the received output power.

CHAPTER 4

RESULTS AND DISCUSSION



4.1 VLC Simulation Result

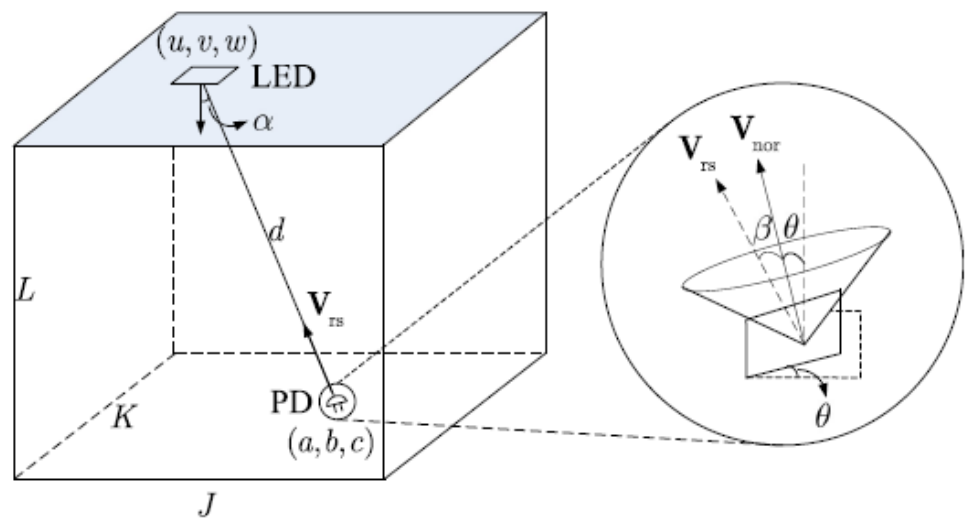


Figure 15: LED array and distribution of illuminance for a single transmitter

Imagine the conventional indoor VLC system represented in Figure 15 with a single LED and a single PD. The room's dimensions are set to $J \times K \times L$, which is $4 \times 4 \times 2$ m. The transmitter is an LED that is mounted in the centre of the ceiling. The LED's location is set to be $[u, v, w]$, which is $[2, 2, 2]$. The PD is deployed as the receiver on a horizontal plane with the coordinates $[a, b, c]$. The PD can be positioned anywhere on the receiver plane, and its direction can be changed by tilting at an appropriate angle. Each individual LED may be considered as a point light source, with a well-defined radiation footprint, and its radiation pattern can be visualised as a function of the solid angle in three-dimensional space. The received optical power is highest at $\phi = 0$ and lowest at $\phi = \phi_{Max}$ for each cell depicted in which are defined as Figure 8, which are defined as

$$P_{r-Max} = P_t \frac{(m_l+1)A_{PD}}{2\pi H^2} T_S(\psi) g(\psi) \cos(\psi), 0 \leq \psi \leq \psi_{con} \quad (4.1)$$

$$P_{r-Min} = P_t \frac{(m_l+1)A_{PD}}{2\pi d_{Max}^2} \cos^{m_l}(\phi_{Max}) T_S(\psi) g(\psi) \cos(\psi), 0 \leq \psi \leq \psi_{con} \quad (4.2)$$

where ϕ_{Max} is the maximum irradiance angle and d_{Max} is the corresponding maximum distance between the transmitter and the receiver within a cell.

Lambertian emission is used to model the channel gain in indoor VLC.

$$h = \frac{(m+1)A}{2\pi d^2} \cos^m(\alpha) \cos(\beta) \quad (4.3)$$

where $m = -\ln 2 / \ln(\cos \Phi_{1/2})$ is the Lambertian order, and $\Phi_{1/2}$ is the semi-angle at half power of the LED, A is the receiver's physical area, d is the transceiver distance, α is the LED's irradiance angle, and β is the PD's incidence angle.

The utilisation of a broad divergence angle LED is a practical approach to obtain comprehensive coverage in a VLC system. However, large divergence angles might result in an increase in multipath-induced Inter-Symbol Interference (ISI), drastically reducing the maximum data rate for transmission. The divergence angles of LEDs must be carefully adjusted to overcome this limitation and obtain a higher data transmission rate and a better uniform optical power distribution. This is because the irradiance angle and incidence angle are dependent on the receiver's location in the room. SNR values are calculated for a variety of incidence and irradiance angles. The highest signal-to-noise ratio is obtained when the transmitter and receiver are placed in-line. Figure 16 illustrates the performance graphs of SNR.

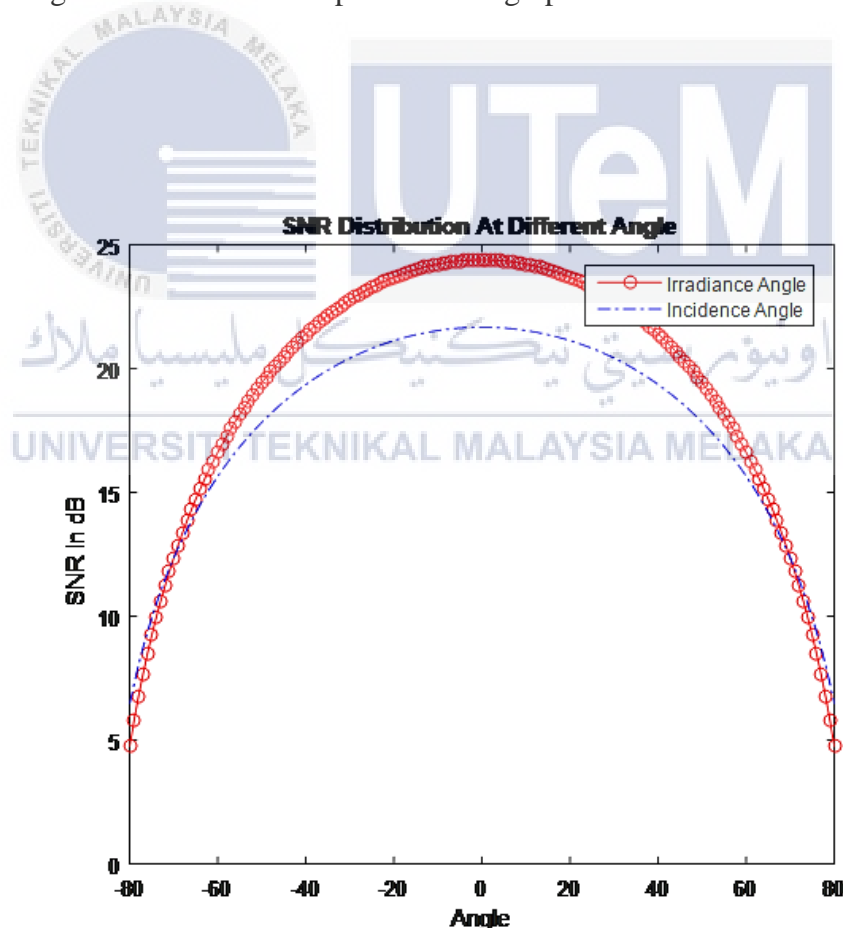


Figure 16: Performance graphs of SNR

As illustrated in Figure 16, FOV affects the performance of the VLC system. SNR values can be determined for various transmitter FOVs. Consider that the receiver is in direct communication with the emitter; from the FOV versus SNR graph for the transmitter is given in Figure 16, a transmitter's FOV should be set above 50 to get a high SNR. Another critical element is that the highest SNR is reached at a FOV of 90. Therefore, to obtain a strong signal, the irradiance angle and incidence angle must be less than 45 degrees while the FOV of the transmitter should always be more than 50 to get maximum SNR.

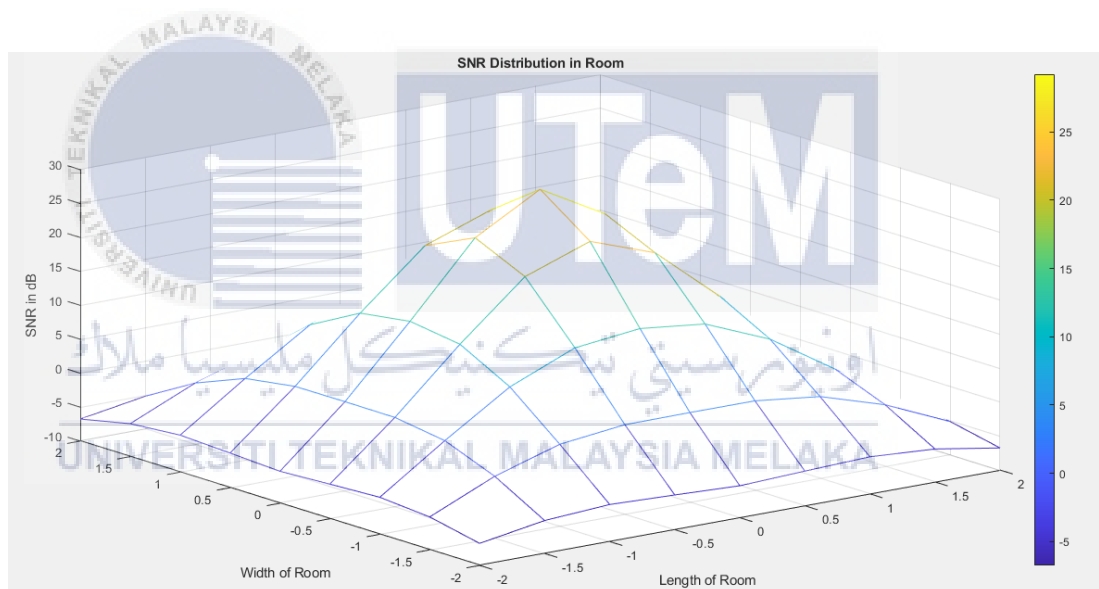


Figure 17: SNR Distribution in the room

SNR can be utilised to indicate the quality of a communication link in OWC. SNR is used to determine the VLC link's capacity. The optical signal-to-noise ratio (SNR) can be defined as the ratio of the average signal power received to the ambient noise. Based on the graph in Figure 16, the FOV value for the transmitter is set at 70° while the FOV value for receiver is set at 90° . Figure 17 shows the SNR Distribution in 4m x

4m x 2m room. The maximum SNR is observed close to the centre of the room. The maximum SNR 29.2 dB is observed at the centre, while a minimum of -6.7dB is observed at the corners.

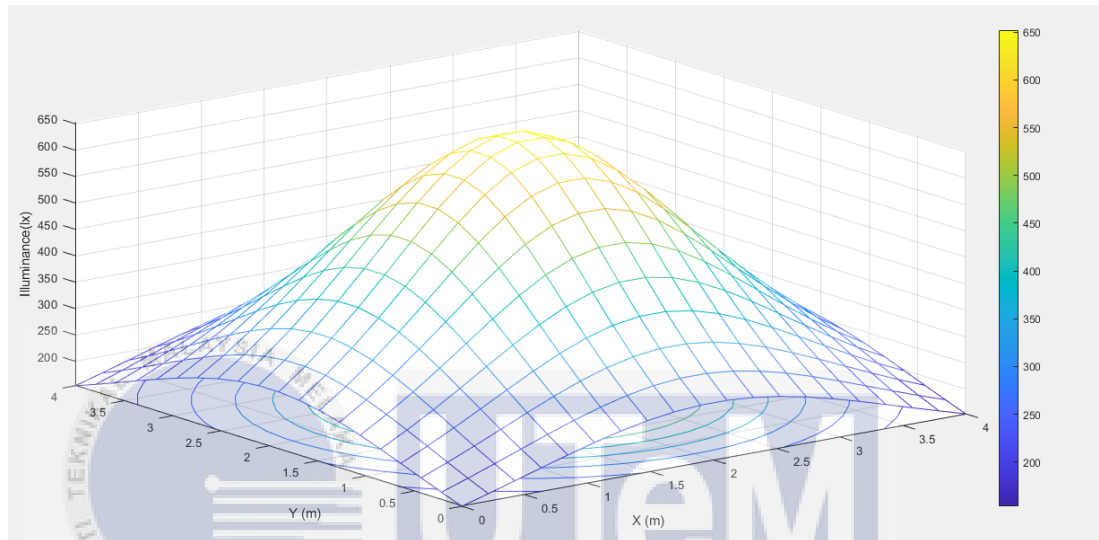


Figure 18: Pattern of illumination for a single LED transmitter

The pattern of illumination for a single LED transmitter with a semi-angle, half-power of 70° is shown in Figure 18, assuming no extra light is reflected from the surrounding walls. ISO defines sufficient illuminance as being between 3000 and 1500 lx. It was observed that the illuminance is greatest in the centre and diminishes toward the margins. The maximum luminous flux value is 652 lx in the centre of the room, while the minimum value is 250 lx at the periphery. As a result, the LED bulbs with the specifications employed in this simulation can provide an adequate illumination level.

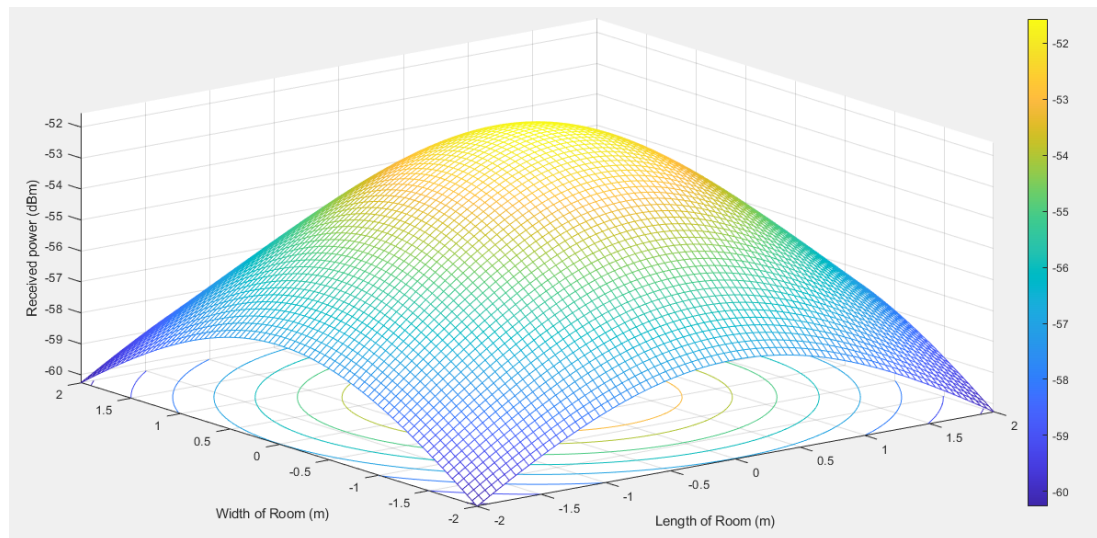


Figure 19: Received power distribution

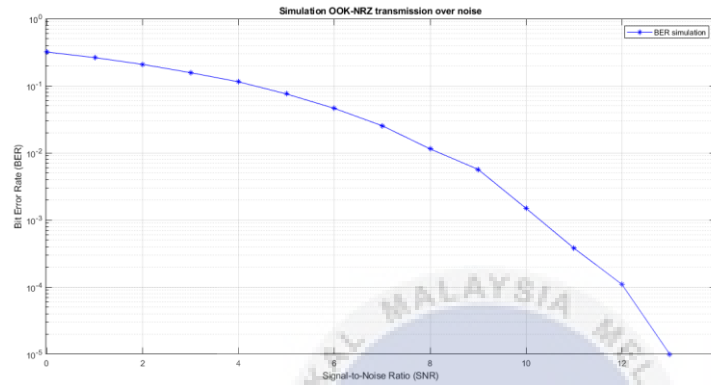
The power distribution seems to be symmetrical due to the symmetry of the room and the location of the transmitters. The high received power is generated at the central spots, collecting the most energy as shown in Figure 19. The greatest power received is -51dBm. With a received power of -60dBm, the received power drops as the PD location moves further away.

UNIVERSITI TEKNIKAL MALAYSIA MELAKA

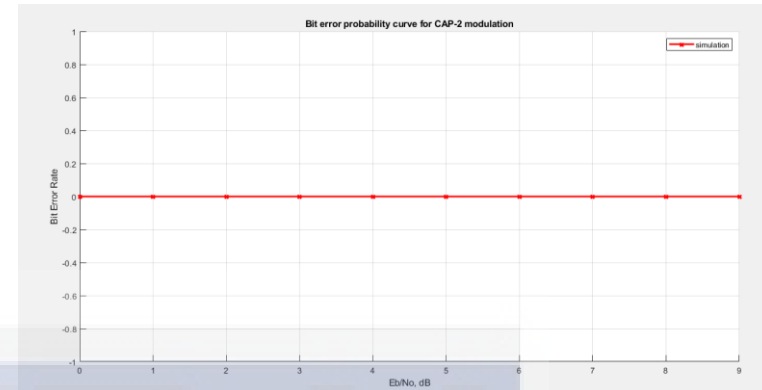
4.2 Performance Evaluation

4.2.1 BER analysis

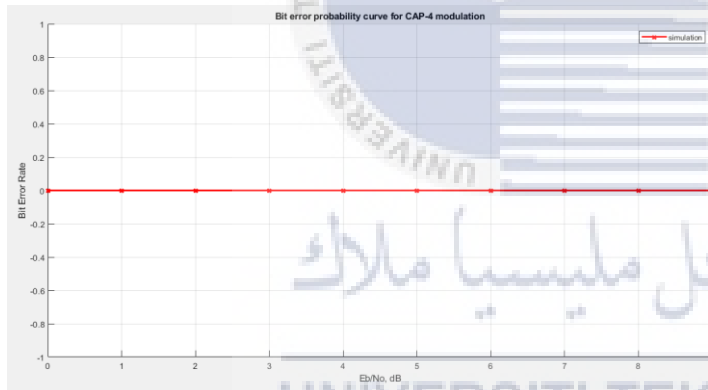
BER is a commonly used indicator of system performance in wireless communications. BER is the number of bits collected from the data stream of the communication channel that compensate for noise errors. Thus, the BER curve can be used to illustrate a digital communication system's performance. The E_b/N_0 ratio is proportional to the signal to noise ratio (SNR), taking the bit rates of the various constellations into consideration.



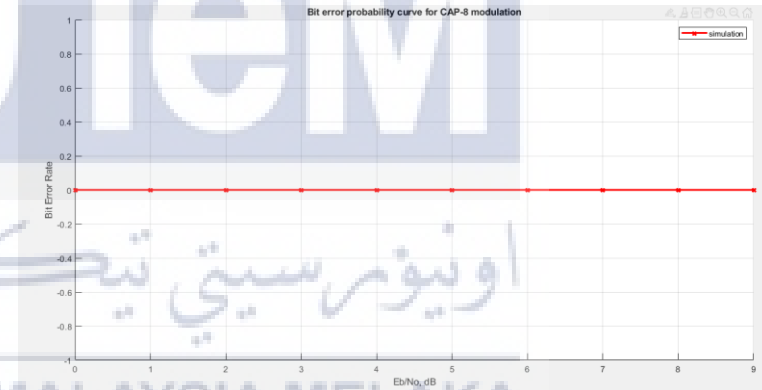
OOK Modulation



CAP- 2 Modulation



CAP- 4 Modulation



CAP- 8 Modulation

Figure 20: BER graph for (a) OOK, (b) CAP-2, (c) CAP-4, (d) CAP-8

From Figure 20, the bit error rate graph observed that as more bit signals are sent out for OOK modulation, the bit error rate increases. However, there is no bit error rate for CAP modulation as there is no distance set in simulation. Therefore, perfect transmission is simulated.

4.2.2 Scatter Plot analysis

A scatter plot or constellation diagram is employed to view the constellation of a digitally modulated signal.

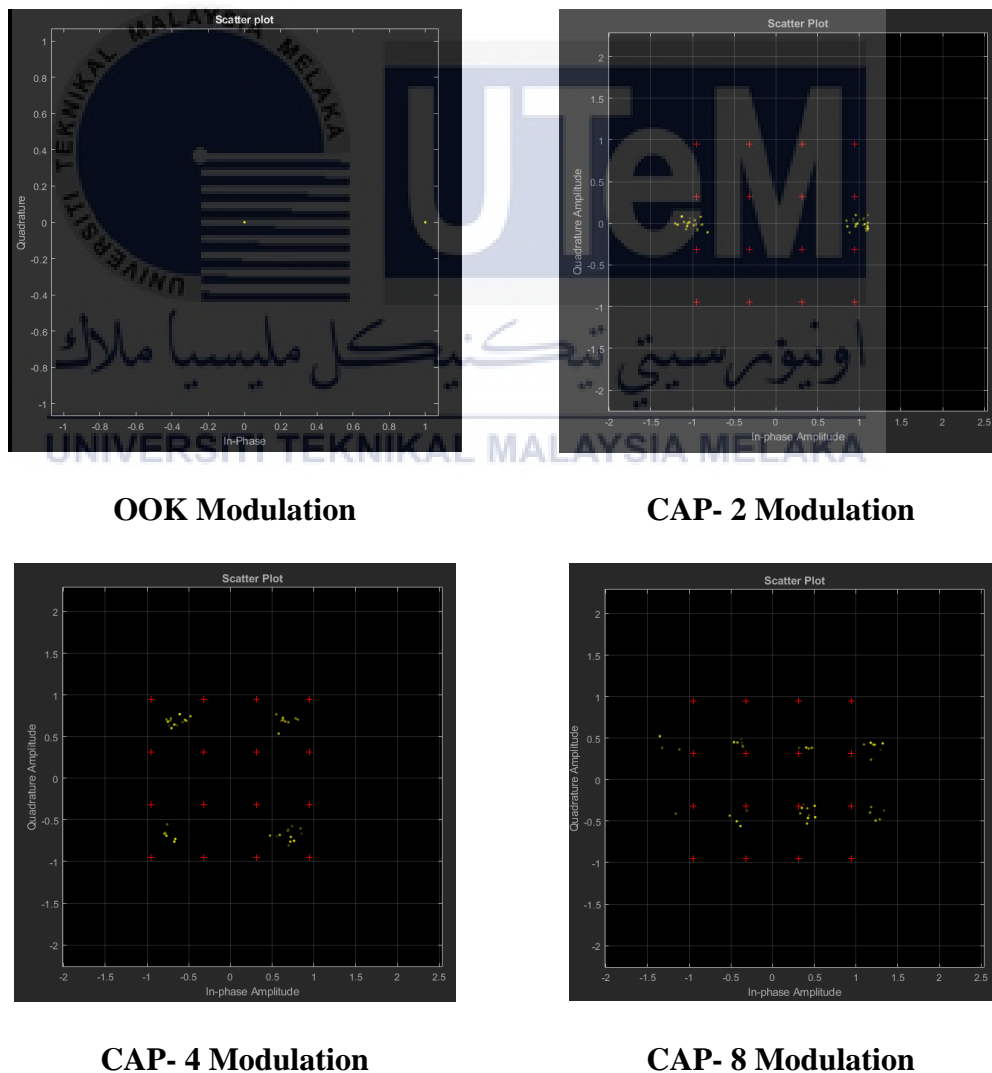


Figure 21: Scatter Plot for (a) OOK, (b) CAP-2, (c) CAP-4, (d) CAP-8

In terms of scatter plots, from Figure 21, it can be observed that as the CAP modulation number increases, the scatter plot also increases. In OOK modulation, logic zero is denoted by lower amplitude, while logic one is denoted by a greater amplitude. In OOK modulation, there is no carrier involved during the transmission of logic zero. Rather than that, the carrier is transmitted during logic one transmission. As a result, the OOK modulation transmitter enters the IDLE state during logic "zero" transmission. Therefore, it is plotted at point 0,0, while logic one is plotted at 1,0. The constellation points in QAM for CAP modulation are typically placed in a square grid with uniform vertical and horizontal spacing. Upgrading to a higher-order constellation permits the transmission of additional bits per symbol. Nonetheless, in attempt to conduct a fair assessment, the constellation's mean energy must remain constant. As a result, points will be closer together and hence more prone to noise and other forms of contamination, as we see in the eyes diagram of CAP-8 compared to CAP-2 or 4.

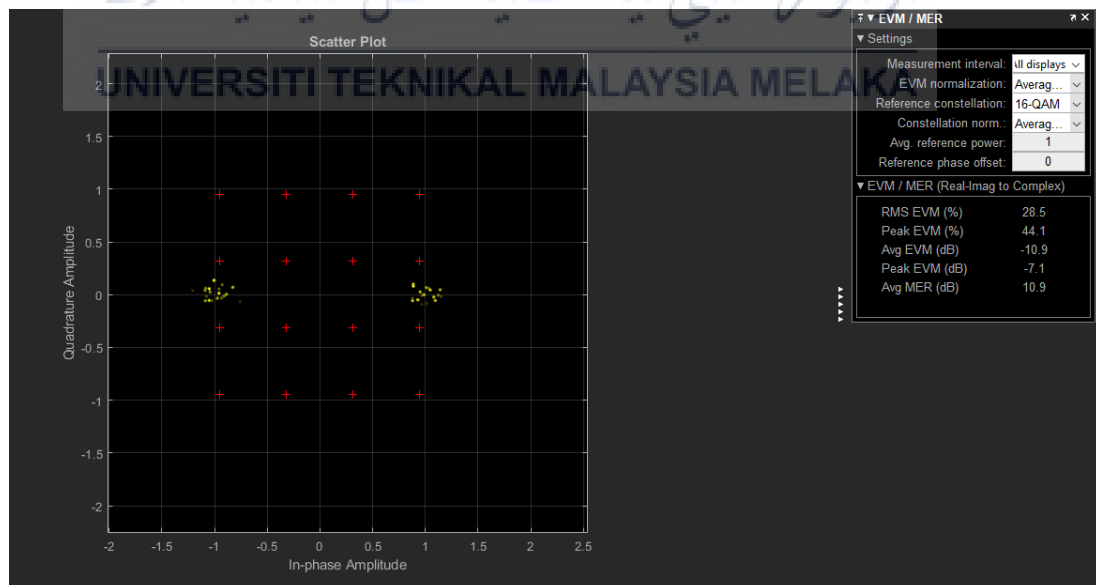


Figure 22: Scatter plot for CAP-2 with signal quality measurement

The scatter plot can be used to determine the signal's quality parameters, such as modulation error ratio (MER) and error vector magnitude (EVM), as shown in Figure 22. The EVM would be used to determine the performance of a digital signal transmitted by the transmitter and received by the receiver, as well as the distance between the points from their desired locations. Every constellation point pointing in the desired direction will be displayed in the received signal. While the MER is used to determine the performance of a digital radio transmitter or receiver employing digital modulation such as QAM, the power received is utilised to determine the loss measures and the power from a source or present at a receiver. The QAM is similar to the CAP in that it allows for multiple levels and modulation in several dimensions. In contrast to QAM, the CAP does not require the creation of sinusoidal signals at both ends, at the transmitter and receiver. Additionally, CAP can be used to modulate in more than two dimensions if orthogonal pulse forms can be discovered.

Table 6: Comparison of the Modulation scheme for EVM, MER and Output Power

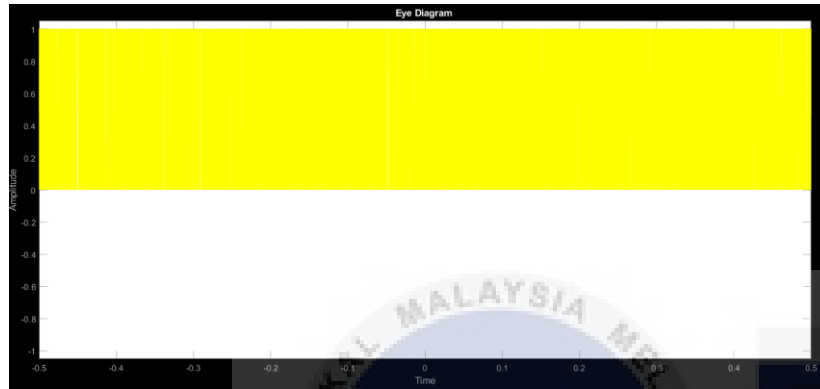
Modulation	EVM (dB)	MER (dB)	Average power (dBW)
OOK	Unable to be retrieved	Unable to be retrieved	Unable to be retrieved
CAP-2	-10.9	10.9	0.1316
CAP-4	-9.6	11.3	5.45
CAP-8	-11.9	9.8	12.42

Scatter plot in Figure 21 shows, it can be observed that the EVM of CAP-4 is the best while the EVM of CAP-8 measures the worse of a digital signal of the transmitter and receiver. This says that CAP-8 has the least ideal scatter plot location than CAP-2 and CAP-4. In terms of MER, CAP-4 has the best reading value compared to CAP-2 and CAP-8. However, CAP-8 records the least reading for MER. In terms of power received, CAP-8 has the highest reading of 12.42dBW compared to other CAP modulation. From Table 6, it can be concluded that CAP-4 record the best reading value overall compared to other CAP modulation.

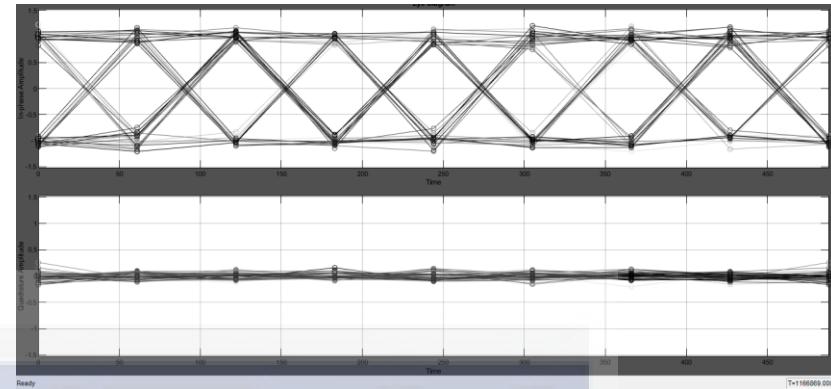
4.2.3 Eye Diagram analysis

In digital communications, an eye diagram illustrates the effect of noise on system performance.

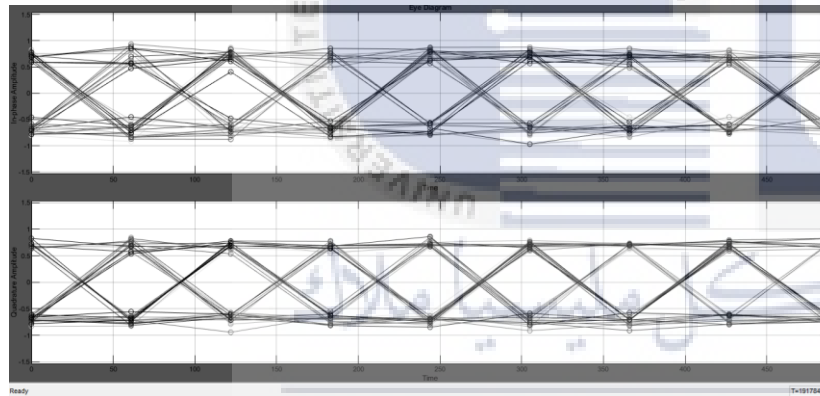
Eye diagram in Figure 23 shows, for OOK modulation, we can see that the eye diagram is significantly distorted due to many input bits. In terms of the eye diagram, it was noted that CAP modulation offers a better visual representation of how noise could affect system performance than OOK modulation. However, CAP-4 offers a better eye diagram because the quality of the in-phase signal and quadrature signal is better than CAP-2 and CAP-8.



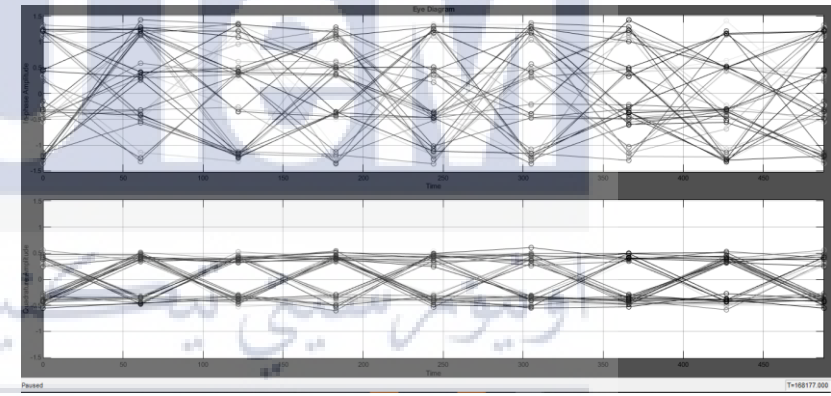
OOK Modulation



CAP- 2 Modulation



CAP- 4 Modulation



CAP- 8 Modulation

Figure 23: Eye diagram for (a) OOK, (b) CAP-2, (c) CAP-4, (d) CAP-8

4.3 Comparison Between CAP and OOK modulation

From the result above, a comparison between CAP modulation and OOK modulation can be made for the VLC system. In BER analysis, CAP modulation records a better result than OOK modulation. This is because, as the input bit rate increases in OOK modulation, the output bit error also increases. However, for CAP modulation, perfect transmission is simulated with zero error.

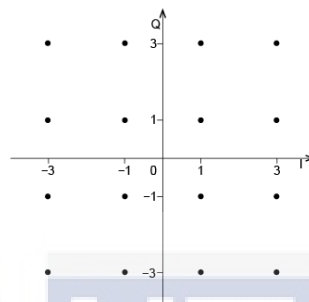


Figure 24: QAM's Constellation diagram

For scatter plot analysis, OOK modulation only has two states that allow for the transmission of either a 0 or a 1. However, numerous alternative points can be used with QAM, each with its defined phase and amplitude values, as shown in Figure 24. QAM, which doubles the number of states to four, results in a symbol with two bits. The number of bits per symbol can be raised further by increasing the constellation's size. This is what is referred to as a constellation diagram. Different values are assigned to the various places, allowing a single signal to transport data at a considerably greater rate. The number of bits per symbol is equal to the log base 2 of the number of constellation points. From Table 7, it can be observed that OOK and CAP-2 carry the least bits per symbol, which is 1 while CAP-8 carry the highest bit per symbol of 3. Therefore, from the scatter plot it can be said that CAP-8 is the best

as it can contain more bits of data per symbol compared to OOK and CAP-2 and CAP-4 modulation. It is also worth noting that increasing the data rate of a link by using a higher-level CAP format is possible.

Table 7: Bit per Symbol comparison

Modulation	Bits per Symbol
OOK	1
CAP- 2	1
CAP-4	2
CAP-8	3

EVM and MER can also be determined from a scatter plot. Unfortunately, EVM and MER for OOK modulation cannot be retrieved. This is because due to limitation in MATLAB coding or MATLAB functions for figure plotted out with coding. But for CAP modulation, EVM of CAP-4 is the best while the EVM of CAP-8 measures the worse of a digital signal which may be due to rectangular, rather than the square shape of the constellation that affects the performance of signal transmitted. For MER, CAP-4 still records the highest reading compared to other CAP while CAP-8 records the least MER reading. This can be said that CAP-8 has the least favourite performance of a digital transmitter or receiver employing digital modulation. However, CAP-8 records the highest power received, meaning it has the most negligible power loss of signal at the receiver. In conclusion, the performance of transmitter and receiver in terms of EVM and MER, CAP-4 will be recommended even though CAP-8 has better output power.

For the eyes diagram, with a large input bit, OOK modulation recorded a very distorted signal which CAP modulation provides a better eyes diagram. This also proves that OOK modulation is not very good with large input data compared to CAP modulation. However, CAP-4 provides a superior eye diagram due to the superior quality of the in-phase and quadrature signals compared to CAP-2 and CAP-8. In conclusion, CAP modulation is better compared to OOK modulation.

4.4 Applications & Commercialization Potential

As the vision of IR4.0 is coming nearer and nearer, the VLC system can assist in resolving the radio frequency (RF) communications spectrum crunch. This contributes to meeting the increased desire for high-speed communication connections among electronics products, sensors, and infrastructure. Furthermore, this project has commercial value, especially in the communication and data transmission field, as it offers high-speed wireless communication as a complementary solution for overcrowded RF and WIFI systems.

4.5 Sustainability & Environmentally Friendly

This project is considered a green technology because the component used (LED) in the project is an efficient lighting source and consumes less electricity than the typical fluorescent light. In other words, VLC technology helps in the reduction of hazardous gases emission. This is because CO₂ and other gases from the electrical energy generated from coal, gas, oil, and nuclear products are reduced as less electricity is consumed.

CHAPTER 5

CONCLUSION AND FUTURE WORKS

5.1 Conclusion

The future of visible-light communication technology is exceptionally bright. This invention addressed the issue of incorporating visible-light communication technology into existing infrastructure without requiring significant alterations. It is a fast-growing part of the communication industry, and it is simply implemented at a low cost. At the end of this project, all the objectives in this project were met. In the thesis, a room with the parameters mentioned in Table 5 is simulated and calculated the illumination parameters of the room for a single-LED array. Other than that, the SNR for the room is also plotted out to determine the quality of a communication link in the room. Next, using CAP modulation, LED's bandwidth limitation can be overcome in the VLC system. In BER analysis, CAP modulation records a better result than OOK modulation. This is because, as the input bit rate increases in OOK modulation, the output bit error also increases. The scatter plot can be used to determine the signal's quality parameters, such as modulation error ratio (MER) and

error vector magnitude (EVM). It can be concluded that the EVM of CAP-4 (-9.6dB) is the best while the EVM of CAP-8 (-11.9dB) measures the worse of a digital signal of the transmitter and receiver. This says that CAP-8 has the least ideal scatter plot location than CAP-2 and CAP-4. In terms of MER, CAP-4 (11.3dB) has the best reading value compared to CAP-2 (10.9dB) and CAP-8 (9.8dB). However, CAP-8 records the least reading for MER. In terms of power received, CAP-8 has the highest reading of 12.42dBW compared to other CAP modulation. Therefore, it can be concluded that CAP-4 record the best reading value overall compared to other CAP modulation. For bit per symbol, it can be concluded that OOK and CAP-2 carry the least bits per symbol, which is 1 while CAP-8 carry the highest bit per symbol of 3. Therefore, from the scatter plot it can be said that CAP-8 is the best as it can contain more bits of data per symbol compared to OOK and CAP-2 and CAP-4 modulation. For the eyes diagram, with a large input bit, OOK modulation recorded a very distorted signal which CAP modulation provides a better eyes diagram. This also proves that OOK modulation is not very good with large input data compared to CAP modulation. However, CAP-4 provides a superior eye diagram due to the superior quality of the in-phase and quadrature signals compared to CAP-2 and CAP-8. In conclusion, CAP modulation is better compared to OOK modulation in term of eye diagram. Subsequent it can be concluded that the system's performance evaluation using CAP modulation is better than OOK modulation in terms of eyes diagram analysis and BER analysis. Therefore, it can be concluded that CAP modulation is better than OOK modulation. Thus, CAP modulation is suitable for indoor VLC system which use LED as an optical source

5.2 Future Work

While the project's objectives have been met, the suggestions for future work are proposed to supplement the work detailed in this thesis.

Recently, there has been new research going on VLC for implementing Artificial intelligence to detect the device's presence and activate the lights in the nearest position. This technology can be used to check the best lightening device based on the illumination and change the data received from one LED to another without losing the signal.

Along with the limited bandwidth generated by the LEDs used in VLC systems, nonlinearities induced by the LEDs add another layer of complexity to VLC systems. These nonlinearities are produced by the LEDs' limited dynamic range and become crucial when using a very high PAPR modulation method such as OFDM since they result in signal clipping, resulting in reduced SNR and higher BER levels. m-CAP is not immune to these phenomena in this environment, as it does exhibit elevated PAPR values. Thus, as a new scheme, it will be interesting to study the extent to which PAPR affects the performance of m-CAP compared to other well-known modulation schemes (e.g., OFDM), as well as potential solutions to this issue.

REFERENCES

- [1] Z. Ghassemlooy, W. Popoola, and S. Rajbhandari, *Optical Wireless Communications*. 2019.
- [2] R. Mueller-Mach, G. O. Mueller, M. R. Krames, and T. Trottier, "High-power phosphor-converted light-emitting diodes based on III-nitrides," *IEEE J. Sel. Top. Quantum Electron.*, vol. 8, no. 2, 2002, doi: 10.1109/2944.999189.
- [3] C. M. Bourget, "An introduction to light-emitting diodes," in *HortScience*, 2008, vol. 43, no. 7, doi: 10.21273/hortsci.43.7.1944.
- [4] A. Eslami, S. Vangala, and H. Pishro-Nik, "Hybrid channel codes for efficient FSO/RF communication systems," *IEEE Trans. Commun.*, vol. 58, no. 10, 2010, doi: 10.1109/TCOMM.2010.082710.090195.
- [5] Y. Tanaka, T. Komine, S. Haruyama, and M. Nakagawa, "Indoor visible light data transmission system utilizing white LED lights," *IEICE Trans. Commun.*, vol. E86-B, no. 8, 2003.
- [6] C. V Forecast, "Cisco visual networking index: Global mobile data traffic forecast update, 2016–2021 white paper," *Cisco Public Inf.*, 2017.
- [7] H. Burchardt, N. Serafimovski, D. Tsonev, S. Videv, and H. Haas, "VLC:

- Beyond point-to-point communication,” *IEEE Commun. Mag.*, vol. 52, no. 7, 2014, doi: 10.1109/MCOM.2014.6852089.
- [8] S. Wu, H. Wang, and C. H. Youn, “Visible light communications for 5G wireless networking systems: From fixed to mobile communications,” *IEEE Netw.*, vol. 28, no. 6, 2014, doi: 10.1109/MNET.2014.6963803.
- [9] D. Karunatilaka, F. Zafar, V. Kalavally, and R. Parthiban, “LED based indoor visible light communications: State of the art,” *IEEE Commun. Surv. Tutorials*, vol. 17, no. 3, 2015, doi: 10.1109/COMST.2015.2417576.
- [10] J. M. Kahn, “Wireless infrared communications,” *Proc. IEEE*, vol. 85, no. 2, 1997, doi: 10.1109/5.554222.
- [11] J. Vučić *et al.*, “230 Mbit/s via a wireless visible-light link based on OOK modulation of phosphorescent white LEDs,” 2010, doi: 10.1364/ofc.2010.othh3.
- [12] N. Fujimoto and S. Yamamoto, “The fastest visible light transmissions of 662 Mb/s by a blue LED, 600 Mb/s by a red LED, and 520 Mb/s by a green LED based on simple OOK-NRZ modulation of a commercially available RGB-type white LED using pre-emphasis and post-equalizing techniques,” 2014, doi: 10.1109/ECOC.2014.6963895.
- [13] Y. Tanaka, T. Komine, S. Haruyama, and M. Nakagawa, “Indoor visible communication utilizing plural white LEDs as lighting,” in *IEEE International Symposium on Personal, Indoor and Mobile Radio Communications, PIMRC*, 2001, vol. 2, doi: 10.1109/PIMRC.2001.965300.

- [14] S. Kitano, S. Haruyama, and M. Nakagawa, "LED road illumination communications system," in *IEEE Vehicular Technology Conference*, 2003, vol. 58, no. 5, doi: 10.1109/vetecf.2003.1286302.
- [15] E. F. Schubert, *Light-emitting diodes, second edition*, vol. 9780521865388. 2006.
- [16] T. Kishi, H. Tanaka, and Y. Umeda, "A high speed LED driver for visible light communications with drawing out remaining carriers by a CMOS inverter," 2011.
- [17] A. H. Abdolhamid and D. A. Johns, "Comparison of CAP/QAM architectures," in *Proceedings - IEEE International Symposium on Circuits and Systems*, 1998, vol. 4, doi: 10.1109/iscas.1998.698823.
- [18] W. O. Popoola, Z. Ghassemlooy, and B. G. Stewart, "Pilot-assisted PAPR reduction technique for optical OFDM communication systems," *J. Light. Technol.*, vol. 32, no. 7, 2014, doi: 10.1109/JLT.2014.2304493.
- [19] S. Dimitrov and H. Haas, *Principles of LED light communications: Towards networked Li-Fi*. 2015.
- [20] G. Stepniak and J. Siuzdak, "Experimental investigation of PAM, CAP and DMT modulations efficiency over a double-step-index polymer optical fiber," *Opt. Fiber Technol.*, vol. 20, no. 4, 2014, doi: 10.1016/j.yofte.2014.04.005.
- [21] K. O. Akande, P. A. Haigh, and W. O. Popoola, "On the Implementation of Carrierless Amplitude and Phase Modulation in Visible Light Communication," *IEEE Access*, vol. 6, 2018, doi:

10.1109/ACCESS.2018.2876001.

- [22] G. H. Im, D. D. Harman, G. Huang, A. V. Mandzik, M. H. Nguyen, and J. J. Werner, "51.84 Mb/s 16-CAP ATM LAN Standard," *IEEE J. Sel. Areas Commun.*, vol. 13, no. 4, 1995, doi: 10.1109/49.382153.
- [23] K. O. Akande and W. O. Popoola, "MIMO techniques for carrierless amplitude and phase modulation in visible light communication," *IEEE Commun. Lett.*, vol. 22, no. 5, 2018, doi: 10.1109/LCOMM.2018.2811459.
- [24] K. Werfli *et al.*, "Experimental Demonstration of High-Speed 4×4 Imaging Multi-CAP MIMO Visible Light Communications," *J. Light. Technol.*, vol. 36, no. 10, 2018, doi: 10.1109/JLT.2018.2796503.
- [25] M. A. Khalighi, S. Long, S. Bourennane, and Z. Ghassemlooy, "PAM-And CAP-Based Transmission Schemes for Visible-Light Communications," *IEEE Access*, vol. 5, 2017, doi: 10.1109/ACCESS.2017.2765181.
- [26] G. Stepniak, M. Schuppert, and C. A. Bunge, "Advanced Modulation Formats in Phosphorous LED VLC Links and the Impact of Blue Filtering," *J. Light. Technol.*, vol. 33, no. 21, 2015, doi: 10.1109/JLT.2015.2472575.
- [27] G. Stepniak, L. Maksymiuk, and J. Siuzdak, "Experimental comparison of PAM, CAP, and DMT modulations in phosphorescent white LED transmission link," *IEEE Photonics J.*, vol. 7, no. 3, 2015, doi: 10.1109/JPHOT.2015.2427092.
- [28] F. M. Wu *et al.*, "Performance comparison of OFDM signal and CAP signal over high capacity RGB-LED-based WDM visible light communication," *IEEE*

Photonics J., vol. 5, no. 4, 2013, doi: 10.1109/JPHOT.2013.2271637.

- [29] J. Wei, Q. Cheng, R. V. Penty, I. H. White, and D. G. Cunningham, "400 Gigabit Ethernet using advanced modulation formats: Performance, complexity, and power dissipation," *IEEE Communications Magazine*, vol. 53, no. 2, 2015, doi: 10.1109/MCOM.2015.7045407.
- [30] K. Zhong *et al.*, "Experimental study of PAM-4, CAP-16, and DMT for 100 Gb/s Short Reach Optical Transmission Systems," *Opt. Express*, vol. 23, no. 2, 2015, doi: 10.1364/oe.23.001176.
- [31] J. Shi, J. Zhang, N. Chi, and J. Yu, "Comparison of 100G PAM-8, CAP-64 and DFT-S OFDM with a bandwidth-limited direct-detection receiver," *Opt. Express*, vol. 25, no. 26, 2017, doi: 10.1364/oe.25.032254.
- [32] N. Chi, Y. Zhou, S. Liang, F. Wang, J. Li, and Y. Wang, "Enabling Technologies for High-Speed Visible Light Communication Employing CAP Modulation," *J. Light. Technol.*, vol. 36, no. 2, 2018, doi: 10.1109/JLT.2017.2783906.
- [33] P. A. Haigh, P. Chvojka, S. Zvánovec, Z. Ghassemlooy, and I. Darwazeh, "Analysis of Nyquist Pulse Shapes for Carrierless Amplitude and Phase Modulation in Visible Light Communications," *J. Light. Technol.*, vol. 36, no. 20, 2018, doi: 10.1109/JLT.2018.2869022.
- [34] M. M. Merah, H. Guan, and L. Chassagne, "Experimental Multi-User Visible Light Communication Attocell Using Multiband Carrierless Amplitude and Phase Modulation," *IEEE Access*, vol. 7, 2019, doi:

10.1109/ACCESS.2019.2893451.

- [35] I. N. Osahon, S. Rajbhandari, and W. O. Popoola, "SI-POF Transmission with CAP Modulation and Split-Complex MLP Equalizer," in *IEEE International Conference on Communications*, 2018, vol. 2018-May, doi: 10.1109/ICC.2018.8422551.
- [36] E. Pikasis, S. Karabetos, T. Nikas, P. Chvojka, A. Nassiopoulou, and D. Syvridis, "Comparison of CAP and DFT-spread DMT for high speed transmission over 50m SI-POF," 2016, doi: 10.1109/CSNDSP.2016.7573941.
- [37] N. Bamiedakis, R. V. Penty, and I. H. White, "Carrierless amplitude and phase modulation in wireless visible light communication systems," *Philosophical Transactions of the Royal Society A: Mathematical, Physical and Engineering Sciences*, vol. 378, no. 2169. 2020, doi: 10.1098/rsta.2019.0181.
- [38] S. Di Mauro and A. Raciti, "Analysis and comparison of CFLs and LED lamps," 2015, doi: 10.1109/AEIT.2014.7002055.
- [39] N. Kumar, D. Terra, N. Lourenco, L. Nero Alves, and R. L. Aguiar, "Visible light communication for intelligent transportation in road safety applications," 2011, doi: 10.1109/IWCMC.2011.5982762.
- [40] M. Rudan, *Physics of Semiconductor Devices*. 2015.

LIST OF PUBLICATIONS AND PAPERS PRESENTED



Article

PERFORMANCE EVALUATION OF CARRIER-LESS AMPLITUDE PHASE MODULATION SCHEME FOR INDOOR VISIBLE LIGHT COMMUNICATION (VLC) SYSTEM

Joyce Yew Pei Ling^{1*}, and Zaiton Abdul Mutalip^{2**}

^{1,2} Faculty of Electronics and Computer Engineering, Universiti Teknikal Malaysia Melaka, Melaka, Malaysia

E-mail: *b021820026@student.utem.edu.my, ** zaiton@utem.edu.my

Abstract. According to recent trends, the existing radio frequency (RF) spectrum may be insufficient to fulfill future data demands. The use of visible spectrum for wireless transmission in visible light communication may be a possible alternative to the RF Spectrum Crunch. Investigating the performance of various modulation techniques in VLC is a new field of research. In the VLC system, data is transmitted digitally and represented by turning ON/OFF the LED. Basically, this is done by a modulator. However, based on the evolution of new generation high brightness LED's, the LED's intensity and flickering become the major problem in VLC, which limits the transmission bandwidth and the performance of the system. This project examines carrier-less amplitude phase (CAP) modulation techniques to overcome this problem and proposes a suitable improvement to the system to be used. Within a simulated VLC system, the performance of CAP in terms of eye diagram, BER and scatter plot is examined. The BER for CAP is zero as no distance is set in simulation which allows perfect transmission to be simulated. For scatter plots, it can be observed that as the CAP modulation number increases, the scatter plot also increases. For eye diagram, it was noted that CAP modulation offers a better visual representation of how noise could affect system performance than OOK modulation.

Keywords: Visible Light Communication, Carrier-Less Amplitude Phase Modulation Scheme, Bit of Error, simulation.

ENGINEERING JOURNAL Volume # Issue #

Received Date Month Year

Accepted Date Month Year

Published Date Month Year

Online at <http://engj.org/>

DOI:10.4186/ej.20xx.xx.x.xx

APPENDICES

Appendix A: VLC system room parameters MATLAB simulation coding

```

>> % BASIC PARAMETER REQUIRED %
Incidence = 70*pi/180;
TX_FOV = 70; % Transmitter Field Of View
RX_FOV = 90; % Receivers Field Of View
Tx = [2,2,2]; % Transmitter Location
%Rxp = [2,2]; % Receiver Location
W_Room = 4; % Width of Room
L_Room = 4; % Length of Room
H_Room = 2; % Height Between Transmitter and Receiver
R = 1; % Responsivity of Photodiode
Apd = 1e-4; % Area of PhotoDetector
Rb = 1e6; % Data rate of system
Iamp = 5e-12; % Amplifier Current
q = 1.6e-19; % Electron Charge
Bn = 50e6; % Noise Bandwidth
I2 = 0.5e62; % Noise Bandwidth Factor
PLED = 1; % Power Emitted by LED
index = 1;
HLED = 1;
[W L] = meshgrid(-(W_Room/2) : 0.50 : (W_Room/2)); % Consider Length of Block for Room
xydist = sqrt((W).^2 + (L).^2);
hdist = sqrt(xydist.^2 + HLED.^2);
%D = Tx - Rx;
%d = norm(D);
%Incidence = acos()
A_Irradiance = ((Tx(3)-HLED)./hdist);
%I(index) = Irradiance*180/pi;
%if abs(Incidence <= RX_FOV)

```

```

p = TX_FOV ;
Tx_FOV = (TX_FOV*pi)/180;
% BASIC CALCULATION IN VLC SYSTEM %
% Lambertian Pattern
m = real(-log(2)/log(cos(Tx_FOV)));
% Radiation Intensity at particular point
Ro = real(((m+1)/(2*pi)).*A_Irradiance^m);
% Transmitted power By LED
Ptx = PLED .* Ro;
% Channel Gain ( Channel Coefficient Of LOS Channel )
%Theta=atand(sqrt(sum((Tx-Rx).^2))/H_Room);
HLOS = (Apd./hdist.^2).*cos(Incidence).*Ro;
% Received Power By PhotoDetector
Prx = HLOS.*Ptx;
% Calculate Noise in System
Bs = Rb*I2;
Pn = Iamp/Rb;
Ptotal = Prx+Pn;
new_shot = 2*q*Ptotal*Bs;
new_amp = Iamp^2*Bn;
% Calculate SNR
new_total = new_shot + new_amp;
SNRl = (R.*Prx).^2./ new_total;
SNRdb = 10*log10(SNRl);
%
%           else
%           SNRl = 0;
%           SNRdb = 0;
%
%           end
index = index + 1;
% Plot Graph %
figure;
mesh(W,L,SNRdb);
%mesh(SNRdb);
%ylim([0 30]);
title('SNR Distribution in Room');
xlabel('Length of Room');
ylabel('Width of Room');
zlabel('SNR in dB');
>> |

```


Appendix B: MATLAB coding to calculate the LOS channel gain.

```

>> theta=70; % semi-angle at half power
m=-log10(2)/log10(cosd(theta)); %Lambertian order of emission
P_total=1; %transmitted optical power by individual LED
Adet=1e-4; %detector physical area of a PD
%% Optics parameters
Ts=1; %gain of an optical filter; ignore if no filter is used
index=1; %refractive index of a lens at a PD; ignore if no lens is used
FOV=70*pi/180; %FOV of a receiver
G_Con=(index^2)/sin(FOV); %gain of an optical concentrator
%% Room dimension
lx=4; ly=4; lz=2; % room dimension in meter
h=2; %the distance between source and receiver plane
Nx=lx*20; Ny=ly*20;% number of grid in the receiver plane
XT=0; YT=0;% position of LED;
x=-lx/2:lx/Nx:lx/2;
y=-ly/2:ly/Ny:ly/2;
[XR,YR]=meshgrid(x,y); % receiver plane grid
Dl=sqrt((XR-XT(1,1)).^2+(YR-YT(1,1)).^2+h^2);
% distance vector from source 1
cosphi_A1=h./Dl; % angle vector
%%
H_A1=(m+1)*Adet.*cosphi_A1.^(m+1)./(2*pi.*Dl.^2);
% channel DC gain for source 1
P_rec=P_total.*H_A1.*Ts.*G_Con; % received power from source 1;
P_rec_dBm=10*log10(P_rec);
meshc(x,y,P_rec_dBm);
xlabel('X (m)');
ylabel('Y (m)');

zlabel('Received power (dBm)');
axis([-lx/2 lx/2 -ly/2 ly/2 min(min(P_rec_dBm)) max(max(P_rec_dBm))]);
>>

```